1. Introduction

Persistent infections caused by hepatitis C virus (HCV) occur in 70–80% of acutely infected individuals, the majority of which will develop chronic hepatitis and will be at risk for cirrhosis, end-stage liver disease and/or hepatocellular carcinoma [1]. Antiviral therapy at present is successful in about 50% of patients, but treatment carries significant side effects and is very costly [2]. At present, there are ~17,000 new HCV infections each year in the U.S. [3], making the development of a vaccine against this virus imperative.

The natural variability of HCV, resulting in the coexistence of quasispecies in infected individuals, could be important in hepatitis C pathogenesis [4]. It has been postulated that immune pressure on these variants brings about the selection of escape mutants able to overcome host immune responses [5,6] and establish persistent infection. The greatest genetic variability is observed in the E1 and E2 glycoproteins [7], posing problems for vaccine development and providing potential for escape from vaccine-induced immune responses.

The essential role of neutralizing antibody (nAb) in controlling viral replication during primary or secondary infections is still unclear. High titres are not produced until the chronic phase of the infection [8] and although the induction of nAbs has been associated with clearance of HCV [9,10], it appears such antibodies may not be an absolute requirement [8,11]. However, antibody to surface proteins of HCV can neutralize virus *in vitro* [12,13] and chimpanzee vaccine studies using recombinant envelope glycoproteins (rE1E2) have shown modified infections and increased rates of clearance [14]. Using lentiviral/HCV pseudotype particles bearing HCV E1E2 on the surface [15,16] or cell culture HCV [17,18] patient plasma samples and monoclonal antibodies (mAbs) have been identified that are capable of cross-neutralizing a number of different genotypes (GTs) [8,16,19–21]. However, the challenge still remains of how to efficiently induce such antibodies by vaccination with recombinant forms of E1E2 antigen. Often peptide vaccination does not induce antibodies with the desired immunogenic effects and there exists very little information on antibody profiles induced by immunization with rE1E2 or the titres of antibodies to specific neutralization epitopes. In this study we compared and analyzed antibody profiles induced following immunization with HCV rE1E2 proteins produced from Vaccinia (VV) and Sindbis (SIN) virus systems. The quality of antibodies was assessed using peptide scanning and *in vitro* neutralization assays employing cell culture viruses (HCVcc) expressing envelope proteins from 3 different subtypes of HCV (1a (H77), 1b (LB) (accession number HQ110091) and 2a (J6/JFH1)). Using peptide blocking and antibody isolation we found that the most immunogenic epitopes induce non-neutralizing antibodies. We identified three new regions important for neutralization. Two of these regions are type specific; antibodies to the third region, which is 85–95% conserved between GTs, were found to be cross-neutralizing. These data are important for vaccine development and suggest that removing some immunogenic sites from proteins may improve presentation and immune responses to nAb epitopes.

2. Materials and methods

2.1. Ethics statement

These studies were carried out in strict accordance with the recommendations in the Guide for the Care and Use of Laboratory Animals of the National Institutes of Health (NIH). The mouse studies were performed under protocols approved by the SRC VB VECTOR Institutional Animal Care and Use Committee (NIH Office of Laboratory Animal Welfare Number A5505-01). The chimpanzee studies were performed under protocols approved by the CBER Institutional Animal Care and Use Committee (PHS Animal Welfare Assurance Number A4295-01). All blood collections from chimpanzees were performed under ketamine/xylazine anaesthesia and all efforts were made to minimize suffering. The human samples used in this study were pre-existing, analyzed anonymously and could not be traced back to donor patients. For these reasons the CBER Committee for Research Involving Human Subjects determined that this research was exempt from review under 45 CFR 46.101 (b).

2.2. Sindbis (SIN) and Vaccinia virus (VV) rE1E2 constructs

Recombinant SIN and VV were constructed expressing aa171–715 of GT 1a HCV (H77) with a carboxy terminus 6-HIS tag, as previously described [22,23].

2.3. Production of purified rE1E2 glycoproteins

Proteins were purified by GNL lectin-affinity chromatography (Vector Labs, Burlingame, CA) and a His-Bind Ni2+ column (Novagen, Madison, WI) [23] from infected BHK cells. Specificity and purity (>80%) were determined by Western blotting, using anti-E1 (A4) and/or anti-E2 (A11) mAbs [24], and silver staining of proteins separated on polyacrylamide gels. Peak fractions were pooled for further purification or for use in immunization.

2.4. Deglycosylation of proteins

For deglycosylation proteins were treated with Peptide: N-glycosidase F (PNGase F) (New England Biolabs, Beverly, MA) according to the manufacturer's instructions.

2.5. Animal immunizations

BALB/c mice were intraperitoneally immunized with 5 μg purified rE1E2 in Freund's Complete Adjuvant (CFA) (Sigma, MO). Control mice were injected with PBS + CFA (normal mouse serum). After 30 and 60 days, animals received intraperitoneal booster injections: 5 μg rE1E2 in Freund's Incomplete Adjuvant (Sigma, MO). Final bleeds were performed 3 weeks after the final boosts. The immunization of Ch1587 and Ch1601 with SIN-E1E2 has been previously described [23].

2.6. Biotinylated peptide ELISAs

Assays were performed using biotinylated peptides (20mers overlapping by 12) covering the entire E1E2 region (Mimotopes, Victoria, Australia), as previously described [22].

2.7. Blocking and affinity purification of peptide-specific antibody

Blocking antibody to specific peptides was performed as previously described [22] using 1–5 μg of non-biotinylated peptides in 100 μl of serum. Affinity purification was performed by incubating biotinylated peptides (1–5 μg) with serum, 60 min at room temperature (RT). Streptavidin coated magnetic beads (Dynabeads-M-280, Invitrogen, CA) were blocked with 5% milk/PBS and incubated with peptide/serum samples, 60 min RT. After washing, bound antibody was eluted with 0.2 M glycine–HCl (pH 2.2), 10 min RT, and neutralized immediately with 1 M Tris–HCl (pH 9.1).

2.8. ID50 and ID90 neutralization titres

ID50 and ID90 titres, the titres determined to neutralize 50% and 90% of the virus, respectively [25], were calculated by performing

2-fold dilutions of sera beginning at 1:32 and ending at 1:4096 in complete DMEM. HCVcc (50 ffu/50 μl) stocks were mixed with serum and incubated at 37 °C for 1 h before infection (100 μl/well) of Huh-7.5 cells [26]. Cells were cultured for 3 days then fixed and stained [18]. Neutralizations were performed in duplicate; foci consisting of ≥3 cells were counted as positive. Negative controls were represented by normal mouse serum (NMS); normal human serum (Innovative Research, Novi, MI) and chimpanzee sera obtained prior to immunization/challenge. Titres are expressed as a reciprocal of the dilution calculated to neutralize 50% of the virus. The dilution of sera began at 1:32; if a 1:32 dilution did not reduce infectivity by 50% we assigned what would have been the next lowest dilution to the sample i.e. 1:16.

2.9. Assessing Ig concentrations

The concentration of IgG, IgA and IgM in samples was assessed using Ig ELISA kits for human sera specific for each Ig subclass (Alercheck, MA) according to the manufacturer's instructions. A commercially prepared 5% (50 mg/mL) immune globulin preparation was included as an internal control for IgG testing which returned a value of 45.65 mg/mL [27].

3. Results

3.1. Purification of rE1E2 proteins

The rE1E2 proteins were analyzed at each stage of the purification process by Western blot (Fig. S1A and B). Differences in glycosylation levels of VV and SIN-E1E2 were consistently observed before and after purification. The SIN-E1E2 proteins were incompletely glycosylated, demonstrated by a series of bands on the Western blots (Fig. S1B). This was confirmed through deglycosylation of the Sindbis E1E2 preparation using PNGase F. Following treatment single bands at 20 kDa, 36 kDa and 57 kDa were observed which correspond to the molecular weights of unglycosylated E1, E2 and E1E2, respectively (Fig. S1C). Despite the differences in glycosylation the proteins could be purified to similar levels (>80% pure) as assessed by Coomassie blue or silver staining (data not shown) and showed similar profiles when analyzed under non-reducing conditions (Fig. S1D). From the analysis of non-reduced proteins it appeared that there were more high molecular weight complexes in the SIN-E1E2 preparation compared to VV-E1E2, suggesting a greater proportion of aggregated complexes. Fig. S1D shows staining of the non-reduced proteins with anti-E1 antibody alone and revealed E1 monomers, dimers and aggregates. Using anti-E2 antibody alone for Western blots of non-reduced proteins revealed only high molecular weight aggregates (data not shown).

3.2. Antibody responses in immunized mice

Sera from the VV-E1E2 and SIN-E1E2 immunized mice were designated VV-AB and SIN-AB, respectively. Sera positive for envelope antibodies in ELISA using whole antigen were pooled and further analyzed by Pepscan ELISA. The SIN-AB displayed a narrow recognition profile (Fig. 1A); by end-point titration we identified 4 determinants with titres >1:800 (aa264–318; aa496–515; aa512–547; and aa632–667), whereas 9 determinants were recognized by VV-AB (Fig. 1A) with end-point titres >1:50,000. Each of the 4 regions recognized by SIN-AB was also recognized by VV-AB; SIN-AB displayed a higher titre against one region, aa496–515, the respective titres for SIN-AB and VV-AB against this epitope were calculated as 1:12,800 and 1:3200.

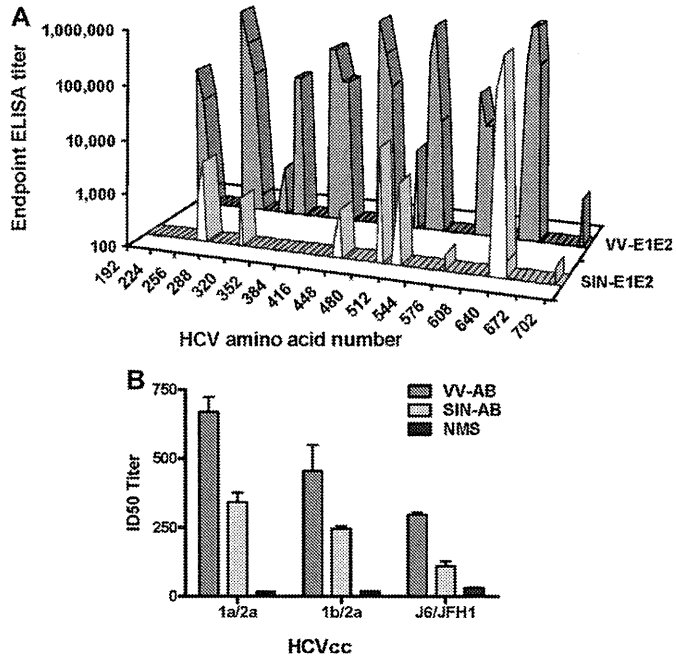

Fig. 1. Pepscan and neutralizing antibody analysis of mouse sera. (A) Pepscan analysis of VV-E1E2- and SIN-E1E2-induced antibodies in mice. End-point titrations were determined on sera starting at 1:200 dilution. End-point titres at each dilution were calculated as the mean OD for NMS + 4 standard deviations. (B) Neutralization of 1a/2a, 1b/2a and J6/JFH1 HCVcc by VV-AB, SIN-AB and normal mouse serum (NMS). Neutralization is expressed as ID50 titre which is the titre calculated to give 50% inhibition of the virus in cell culture. Error bars represent standard error of the mean of replicates within one experiment. Neutralization of HCVcc was performed at least 3 times with similar results.

3.3. In vitro neutralization of HCVcc with mouse sera

ID50 titres were determined against 1a/2a, 1b/2a and 2a (J6/JFH1) HCVcc (Fig. 1B). Despite the broader peptide recognition profile and higher ELISA titres the ID50 titre of VV-AB was only ~2.0-fold higher than SIN-AB against the 1a/2a and 1b/2a HCVcc. Both serum samples were also able to neutralize more than 90% of HCVcc 1a/2a although only at dilutions of ~1:64 and 90% neutralization was not obtained in all assays performed (Fig. S2). For assays where 90% neutralization was obtained the mean ID90 titres against HCVcc 1a/2a for VV-AB and SIN-AB were calculated as 67.5 and 45.9, respectively. In addition, SIN-AB was able to cross-neutralize J6/JFH1 (Fig. 1B), although VV-AB showed an almost 3-fold better cross-neutralization of J6/JFH1 (ID50 = 295) compared to SIN-AB (ID50 = 109).

3.4. ID50 titres of blocked and unblocked mouse sera

In order to assess which determinant-specific antibodies contributed to neutralization we performed blocking assays prior to neutralization and compared the ID50 titre to sera blocked with Flu peptides. ELISA signals were assessed after blocking with Flu or HCV-specific peptides covering the 4 determinants recognized by both SIN-AB and VV-AB. A number of determinants (e.g. aa264–318) were represented by more than one of the over-lapping peptides in the Pepscan therefore all peptides were used for blocking and a reduction in signal against all peptides was verified by ELISA. In all cases peptide blocking reduced the specific ELISA signal substantially (Fig. S3A–H). The same serum samples were then tested in neutralization assays with 1a/2a HCVcc.

Despite substantial blocking of antibodies to the 3 peptides covering the major determinant recognized by both VV-AB and SIN-AB (aa632–667) (Fig. S3G and H) there was little effect

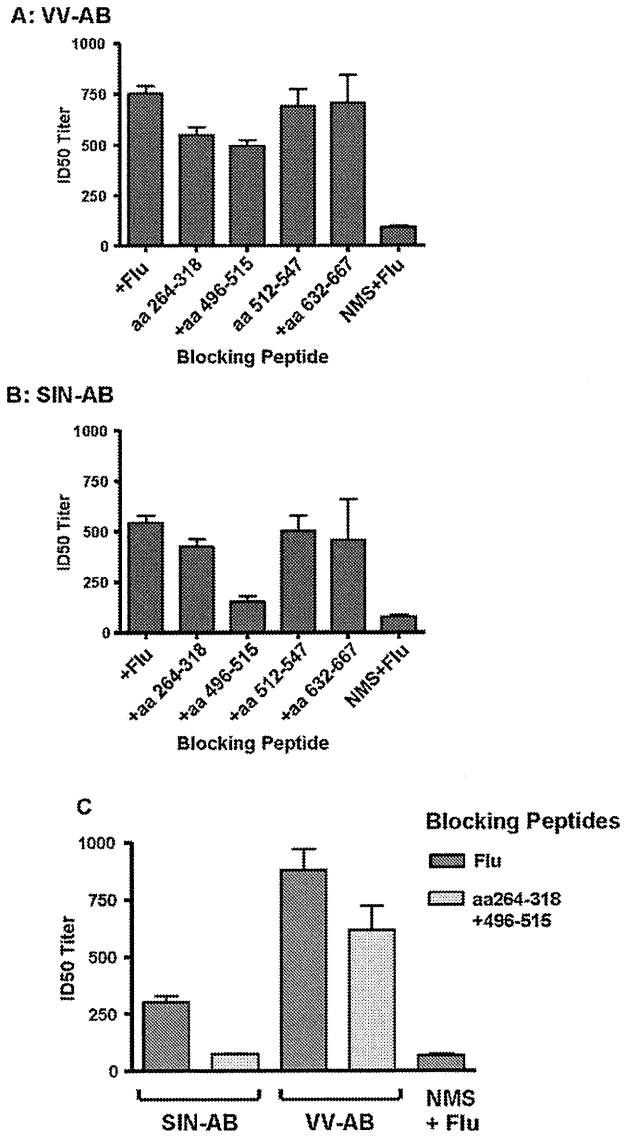

Fig. 2. ID50 titres of mouse sera following blocking with specific and control peptides. (A) VV-AB, (B) SIN-AB, (C) SIN-AB and VV-AB blocked with peptides representing aa264–283, 272–291, 280–318 and 496-515 combined. Error bars represent standard error of the mean of replicates within one experiment. NMS represents normal mouse serum. Experiments were performed at least 3 times with similar results.

on neutralization of 1a/2a HCVcc by either sample, Fig. 2A and B. The ratios of mean ID50 titres for Flu-blocked sera and aa632–667-blocked sera were 1.07 and 1.2 for VV-AB and SIN-AB, respectively. A similar result was obtained using peptides encompassing aa512–547 (Fig. 2A and B), blocking antibodies specific to this region marginally reduced ID50 titres from 753.6 to 691.7 (ratio = 1.1; 8.2% reduction) and from 545.6 to 505.2 (ratio = 1.1; 7.4% reduction) for VV-AB and SIN-AB, respectively. However, blocking SIN-AB with a peptide representing aa496–515 reduced neutralization of 1a/2a HCVcc by 72% from 545.6 to 152.6 (Fig. 2B). Blocking the same peptide-specific antibodies in VV-AB reduced neutralization but to a lesser degree, the ID50 titre decreased 34.1% from 753.6 to 495.9. This is consistent with the lower reactivity of VV-AB to this epitope (Figs. S1A and S3C) and suggests antibodies to aa496–515 play a lesser role in neutralization with VV-AB where antibodies are present that recognize known neutralization epitopes, specifically HVR1 and 412–426, than with SIN-AB where they seem to represent the major neutralizing response. Blocking

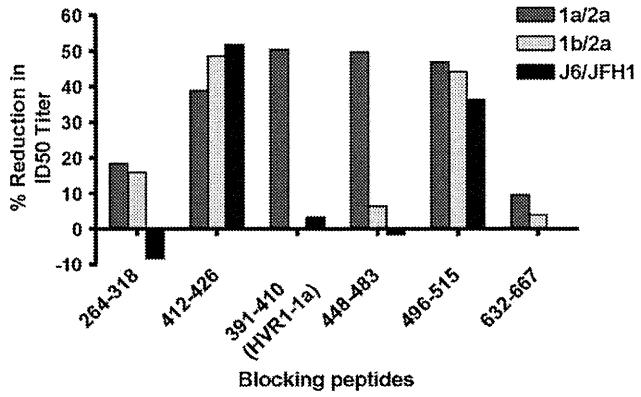

Fig. 3. Percentage reduction in ID50 titres of VV-AB following blocking with specific peptides. 1a/2a, 1b/2a and J6/JFH1 HCVcc were used to test the effects of blocking. Regions blocked are shown on the *X*-axis. Percentage reduction was calculated as ((ID50 of Flu peptide blocked sera – ID50 HCV peptide blocked sera)/ID50 of Flu peptide blocked sera) × 100.

antibodies to aa264–318 also reduced ID50 titres for 1a/2a HCVcc by 27% and 21.7% for VV-AB and SIN-AB, respectively.

These data suggested that the regions aa264–318 and aa496–515 contain neutralization epitopes. In order to assess whether antibodies to these two regions represent the majority of neutralizing activity in SIN-AB we blocked the same serum sample with peptides representing both regions. The ELISA signals were substantially reduced after blocking with the combined peptides (Fig. S4). Blocking SIN-AB with both sets of peptides led to almost complete abrogation of neutralizing activity reducing the ID50 titre to 75.7, similar to that seen for NMS (69.5) (Fig. 2C). However, combining the peptides to block VV-AB did not reduce the ID50 titre beyond that seen when peptides to the individual regions were used, further suggesting that these antibodies do not represent the major neutralizing activity in this preparation.

3.5. *Identification of cross-neutralizing antibodies in mouse sera*

In order to confirm that additional antibodies in the VV-AB preparation have neutralizing activity and to examine the role of antibodies to specific epitopes in cross-neutralization we performed neutralization assays using 1a/2a, 1b/2a and J6/JFH1 HCVcc using blocked and Flu-blocked VV-AB. This serum was shown by Pepscan to contain antibodies to a number of epitopes (Fig. 1A) including hypervariable region 1 (HVR1) (aa390–410) and EPI (aa412–419); a conserved epitope downstream from HVR1. Antibodies to EPI have been shown to be broadly cross-neutralizing [19,20,28]. ELISA signals were substantially reduced after blocking of the VV-AB (Fig. S5). In order to ensure that carry-over peptide from the blocking experiments did not impact viral infection we incubated virus with specific peptides at the concentrations used in the blocking assays and performed a standard infection of Huh-7.5 cells. No impact on infectivity levels was noted (Fig. S6). For clarity the effect of specific blocking on neutralization is shown as % change in ID50 titres relative to the ID50 titre of the Flu treated VV-AB against the same HCVcc (Fig. 3).

Blocking antibodies to aa632–667 had little effect on neutralization of the 3 viruses tested, which is consistent with the data shown in Fig. 2. In addition blocking antibodies to aa200–235, aa312–339 and aa702–721 had little effect on neutralization (data not shown). However, blocking antibodies to aa264–318 resulted in ~20% reduction in the ID50 titre to both 1a/2a and 1b/2a HCVcc but had no effect on the neutralization of J6/JFH1, suggesting the region is not conserved in this GT2a HCVcc. Analysis of the %

Table 1
Percentage identity between 1b (LB) and 2a (J6/JFH1) sequences encoded by the HCVcc used in this study compared to the H77 1a sequence encoded by the 1a/2a HCVcc chimera used in this study.

Amino acid region	% identity	
	1b	2a
264–318	83.3	63.9
412–426	93.3	86.7
391–410 (HVR1)	36.8	36.8
448–483	66.7	44.4
496–515	90	85

identity for this region encoded by each of the HCVcc used in this study supports this as there is higher conservation of this region in the 1b/2a HCVcc chimera (83.3%) than in the J6/JFH1 (GT2a) (63.9%) (Table 1). Blocking antibodies to HVR1 (aa390–410) or aa448–483 substantially reduced the neutralization of 1a/2a HCVcc but did not affect neutralization of 1b/2a or J6/JFH1 as these regions are highly diverse (Table 1). Conversely, blocking aa412–426 (EPI) reduced neutralization of 1a/2a, 1b/2a, and J6/JFH1 by up to 50%. Finally, blocking antibodies to aa496–515 affected neutralization of all 3 HCVcc, this region is conserved between each of the 3 HCVcc viruses studied (Table 1). This data confirms the specificity of the blocking assays and demonstrates that the region aa496–515 represents a new, conserved neutralization epitope.

3.6. Induction of antibodies to aa496–515 in naturally infected or vaccinated patients and chimpanzees

We compared aa496–515 using prototype sequences from GT1–6. The greatest conservation of the GT1a sequence was seen with GT1b (90%) and the greatest diversity was seen with GT2a, GT5a and GT6a (85%) (Fig. 4A). Residues 502–515 were 100% conserved between GTs.

We tested serum samples from vaccinated chimpanzees ($n=2$ [23]); acute phase samples from chimpanzees that cleared HCV ($n=5$, taken at seroconversion [29]); rechallenged animals ($n=3$, taken 2–3 weeks after rechallenge); chronically infected chimpanzees ($n=6$, infected with GT1a (H77) for >3 years) and chronically infected patients (GTs 1b; 2a; 2b; 2a/2c; and 3a viruses ($n=54$)). The vaccinated chimpanzees developed substantial levels of antibody to aa496–515; P/N ratios of 9.2 (Ch1587) and 3.1 (Ch1601) at 1:1000 dilution (Fig. 4B). The remaining samples were tested at 1:100 dilution. None of the chimpanzees that cleared HCV during primary or secondary infections had elevated levels of antibody to aa496–515 while only one of the chronically infected chimpanzees had slightly elevated levels, P/N ratio of 1.9 (Fig. 4C). A small proportion (6/54; 11%) of samples from chronically infected patients had P/N ratios ≥ 2. No specific GT was associated with positive signal; the samples with elevated signals ≥ 3 were derived from patients infected with GT3a. To ensure that the serum samples were reactive in an ELISA all samples were tested against additional peptides when tested for reactivity to peptide 496–515. The majority of the patient samples ($n=45$) were tested in a full Pepscan covering the entire E1 and E2 region; all of these sera reacted with multiple peptides in the Pepscan even when no reactivity was observed with the 496–515 peptide. The remaining chimpanzee and patient samples were screened against a number of additional peptides. Specifically a peptide to 412–426; a peptide to HVR1 (H77, 1a sequence corresponding to the virus that was used to infect the chimpanzees); an NS3 peptide that represents a conserved epitope (aa1026–40) and a core peptide (aa28–42). All samples tested gave positive signals to at least one of these peptides (data not shown).

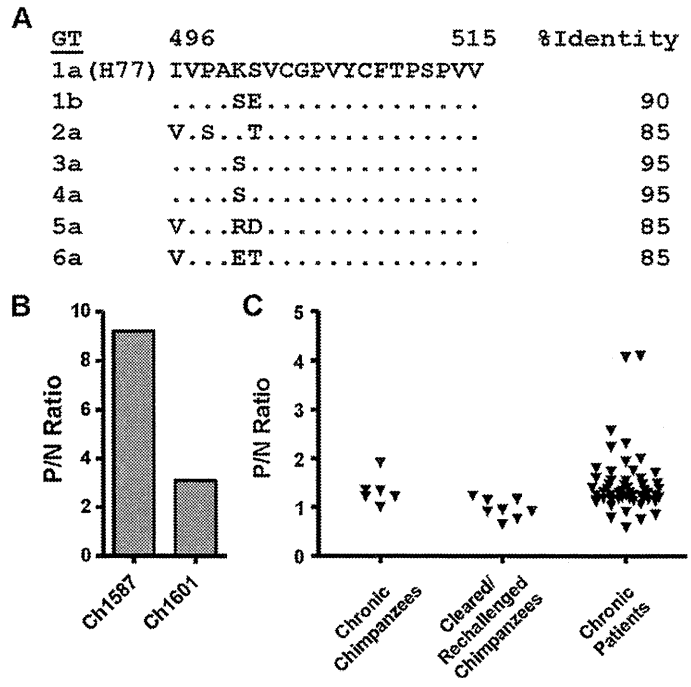

Fig. 4. Conservation of 496–515 sequence and reactivity of patient and chimpanzee sera. (A) Alignment of prototype sequences corresponding to aa496–515 from HCV genotypes 1–6. Sequences were obtained from the Los Alamos HCV Database (http://hcv.lanl.gov). (B) Reactivity of sera from vaccinated chimpanzees to peptide 495–515. Sera were diluted 1:1000. P/N ratio represents the OD of the positive sample divided by the OD of a negative serum sample from the same animal. (C) Reactivity of sera from chimpanzees and patients infected with HCV. Sera were diluted 1:100. For the chimpanzee data P/N ratio represents the OD of the positive sample divided by the OD of a negative serum sample from the same animal. For the patient samples the P/N ratio represents the OD of the test samples divided by the mean OD value of signals from negative human sera.

3.7. Neutralization with antibodies affinity eluted from chimpanzee serum

In order to confirm aa496–515 as a neutralization epitope that can also be recognized by antibody from vaccinees we affinity eluted antibodies from Ch1587 serum and tested the eluate (AB-496) in a neutralization assay. As a positive control in these studies we used a peptide representing the EPI epitope (aa412–426) (AB-412) and as negative controls we used peptides representing aa632–667 (AB-632) and a Flu-M2 peptide. Antibodies from aa632–667 had been shown to be non-neutralizing in our earlier mouse studies (Figs. 2 and 3). The purity and specificity of the eluates were assessed by performing a Pepscan analysis. The affinity eluted samples only recognized the E2-specific peptides used for isolation while a range of peptides from this region were recognized by the unpurified Ch1587 serum (Fig. S7).

As expected the untreated Ch1587-AB (Ch1587-pos) and AB-412 neutralized all three HCVcc (Fig. 5A). In addition, AB-496 was able to neutralize all three HCVcc, with ID50 titres of 202.9, 131.9 and 70.6 against 1a/2a, 1b/2a and J6/JFH1, respectively. The ID50 titres obtained for the negative control eluates, AB-neg and AB-632, were measured as <32 against all HCVcc and assigned titres of 1:16; the next lowest dilution. We did not obtain 90% neutralization at any dilution tested using the Ch1587-pos or the affinity purified antibodies (Fig. S8).

We consistently found that AB-412 had higher ID50 titres than AB-496. To determine whether this was due to better binding of the antibody to the respective epitope or due to higher concentrations of the 412 antibody in the original serum sample leading to more efficient isolation we assessed IgG, IgA and IgM concentrations

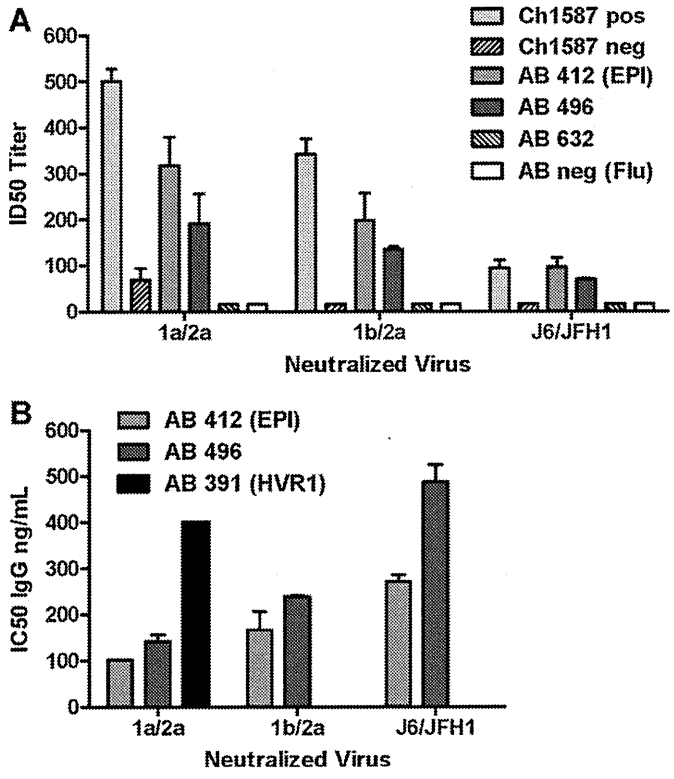

Fig. 5. Neutralization of HCVcc with affinity purified antibody. (A) ID50 titres against 1a/2a, 1b/2a and J6/JFH1 of untreated serum from Ch1587 pre- (Ch1587-neg) and post- (Ch1587-pos) vaccination and affinity purified antibody from Ch1587-pos using specific peptides as noted. AB-neg represents the eluate from Ch1587-pos serum using Flu M2 peptide; AB-412 represents the eluate from Ch1587-pos serum using a peptide representing EPI (aa412–426); AB-632 represents the eluate from Ch1587-pos serum using a peptide representing HCV aa632–651, antibody to this epitope had been shown to be non-neutralizing. (B) IC50 titres of affinity purified AB-412 (EPI), AB-496 and AB-391 (HVR1) against 1a/2a, 1b/2a and J6/JFH1 HCVcc. IC50 titres were calculated as the amount of IgG (ng/mL) required to neutralize 50% of the virus. Error bars represent standard error of the mean of replicates within one experiment. Neutralization assays were performed at least 3 times with similar results.

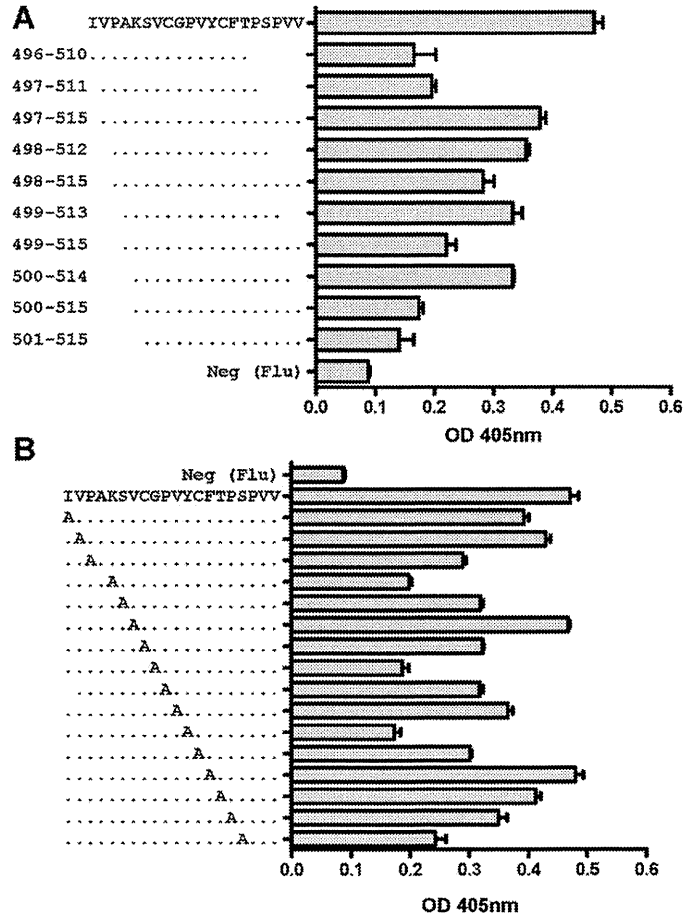

Fig. 6. Mapping essential amino acids in 496–515 epitope. (A) Reactivity of affinity purified AB-496 (diluted 1:100) to overlapping 15mer peptides representing the 496–515 epitope. (B) Reactivity of purified AB-496 (diluted 1:100) to 496–515 peptides containing alanine substitutions. Error bars represent standard error of the mean of replicates within one experiment.

in Ch1587-pos and in each eluate and determined the IC50 titre, the amount of Ig (ng/mL) needed to neutralize 50% of the virus (Fig. 5B). In the unpurified sample (Ch1587-pos) the levels of IgA, IgM and IgG were calculated to be 0.011 mg/mL, 0.188 mg/mL and 65 mg/mL, respectively. For the affinity purified antibodies, AB-496 and AB-412, the signals for IgA and IgM were below the values of the standard curve at 1:50 dilution (i.e. $\leq$0.8 μg/mL in the original undiluted sample) while the amount of IgG was calculated to be ~24 μg/mL for both samples, i.e. at least 300-fold higher. It was concluded that the neutralizing activity in the affinity purified samples was due to IgG antibody; therefore IC50 values are expressed as ng/mL of IgG. For both samples more IgG was needed to neutralize 1b/2a and J6/JFH1 HCVcc than 1a/2a, presumably due to epitope variation. We also found that less of the antibody to aa412–426 was required to neutralize 50% of the virus compared to antibody recognizing aa496–515; the average IC50 titre for AB-412 derived from 2 separate isolations against 1a/2a was calculated as 102 ng/mL, while for AB-496 this was calculated as 142 ng/mL. These values compared to an IC50 titre of 399 ng/mL for an HVR1-specific eluate isolated from the same Ch1587 plasma sample.

3.8. Mapping antibodies to aa496–515 using chimpanzee serum

In order to more precisely map this aa496–515 epitope we performed alanine scanning and synthesized 15mer peptides overlapping by one residue. There were no mutations or truncations that led to complete abrogation of binding. However, using affinity purified AB-496 we found that both the carboxy and amino termini were important for efficient binding of antibody (Fig. 6A; peptides 496–510 and 501–515). These data were confirmed by alanine scanning using peptides with single residue substitutions. Substitutions at the carboxy and amino termini impacted binding (residues 500 and 512) but in addition residues in the centre of the epitope at aa504 and 507 also reduced binding to less than 50% of that obtained using the wild type peptide (Fig. 6B). Similar effects were seen using unpurified Ch1587 serum, VV-AB and SIN-AB against the same mutated peptides (data not shown).

We also performed a full Pepscan analysis of isolated AB-496 using peptides representing both the E1 and E2 regions. We found that in addition to recognizing peptides covering the aa496 region the purified eluate also reacted with 2 peptides in E1 representing aa360–387 (Fig. 7A). This cross recognition was reproducible with several individual AB-496 preparations and when the reverse antibody isolation experiment was performed using peptides representing aa360–387 the purified eluate recognized peptides covering the aa496 region (Fig. 7B). The purified AB-360 was also able to neutralize HCVcc 1a/2a, with an ID50 titre of 1:133, similar to AB-496 purified at the same time (1:178) (Fig. 7C). In terms of sequence similarity the two regions are highly diverse (only ~10% similarity), which excludes the possibility of cross reactivity based upon sequence homology. When comparing charge and hydrophobicity peptide 496 was found to have a net charge of +0.9

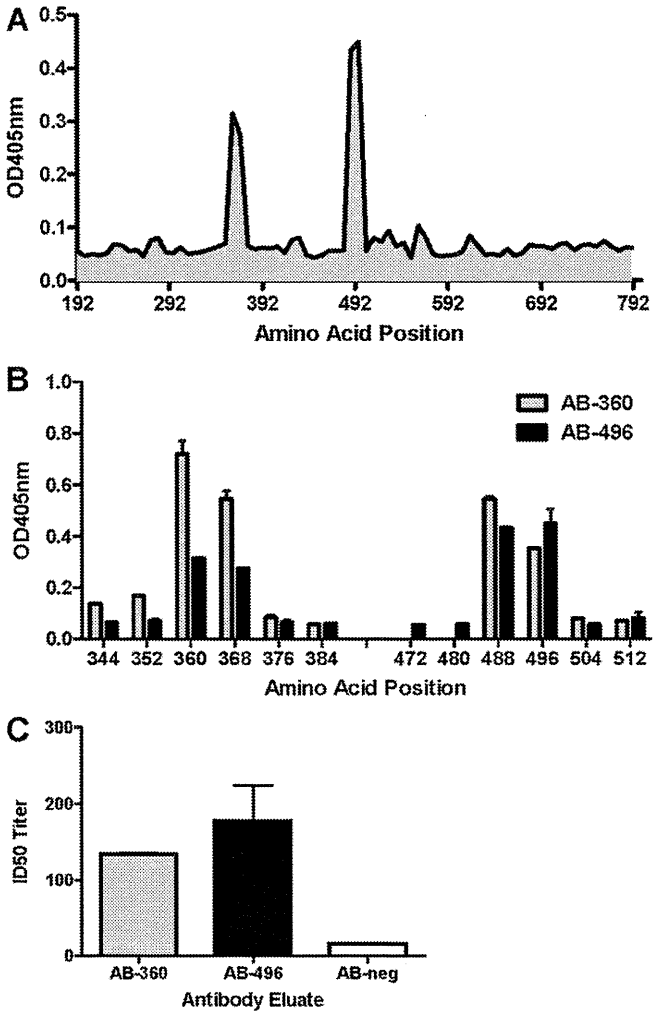

Fig. 7. Analysis of cross reactive region 344–403. (A) E1E2 Pepscan profile of affinity purified antibody AB-496 (diluted 1:400). (B) Cross-reactive ELISA signals obtained for affinity purified antibodies AB-360 and AB-496 when tested against peptides representing aa344–403 and aa472–531. Error bars represent standard error of the mean of replicates within one experiment. Assays were performed three times with similar results. (C) Neutralization of HCVcc chimera 1a/2a using antibody affinity purified with peptides representing aa360–387 (AB-360), aa496–515 (AB-496) and a negative Flu peptide (AB-neg). Error bars represent standard error of the mean of replicates within one experiment.

at pH 7 using a Hopp&Wood analysis while the E1 peptide sequence was found to have a net charge of 0 at the same pH. Both peptides sequences contain 5–6 valine residues but the E1 region is substantially more hydrophobic containing several leucine residues. The reactivity of the E1 peptides was specific to AB-496, no cross reactivity was seen between the peptides and AB-412 or AB-632 (data not shown) therefore the hydrophobic nature of the peptide itself does not seem to be the cause of non-specific reactivity to Ig.

4. Discussion

A large number of nAbs have been identified that can cross-neutralize HCV GTs [8,16,19–21,28,30]. However, the challenge for any HCV vaccine is how to induce such broadly reactive antibodies in vaccinees; during vaccination the use of recombinant proteins or inclusion of adjuvants may not present the same epitopes such that a different repertoire of antibodies is induced. The use of virus-like particles (VLPs) for vaccination may address this issue. However, a chimpanzee study using adjuvanted HCV-VLPs was effective at inducing HCV-specific T-cell immune responses that controlled viral infection but did not induce nAbs and the protection appeared to be wholly T-cell based [31].

We show in this study that the expression system used to produce rE1E2 for immunization may have an impact on the nAb induction. Using Vaccinia- and Sindbis-expressed proteins we found that although both induce an HCV-specific response the VV-AB was broader and more cross-neutralizing than the SIN-AB (Fig. 1). Both types of antigen were expressed in the same cell line, BHK cells, and the same amount and quality of protein were used for immunizations. N-linked glycosylation has been shown to play an important role in folding, activity and immunogenicity for HIV and HCV glycoproteins [32,33]. Analysis of Western blots for both proteins showed that the SIN-E1E2 proteins are not as fully glycosylated as the VV-E1E2 proteins (Fig. S1), possibly due to a higher level of expression in the Sindbis system, which may result in different folding of the protein and therefore different presentation of epitopes to the immune system. Analysis of the proteins in the non-reduced form revealed high molecular weight aggregates in both preparations although the SIN-E1E2 preparation contained a higher amount of aggregated product which would be consistent with a different form of folding (Fig. S1D). Western blots probed with anti-E2 monoclonal antibody alone only revealed high molecular weight aggregates in both preparations with no monomers or dimers detectable (data not shown). This could have been due to the monoclonal antibody poorly recognizing E2 in the non-reduced state or due to aggregation of the majority of E2 complexes in both preparations. It should be noted that the monoclonal antibodies used in our studies were generated against proteins isolated from SDS PAGE gels run under reducing conditions and they do not differentiate between correctly and incorrectly folded proteins. Further characterization of the proteins and responses in individual animals is needed to confirm the cause of these different antigenic responses.

Despite this possible difference in processing or antigenic presentation between the two recombinant proteins, we show in this study that the major immune responses in mice were to non-neutralizing epitopes located between aa512–547 and aa632–667. MAbs isolated from rodents have been previously shown to recognize these regions [16,34,35] and although mAbs mapping between aa524–535 have been found to block binding of E2 to CD81 little or no neutralization was found using pseudotype particles [16,36], which is consistent with our data. However, this region was also found to form part of a conformational epitope recognized by human mAbs able to broadly cross-neutralize HCVcc [30]. This contradiction may be explained by the isolation of the human mAbs from infected patients. When the aa512–547 region is presented by the viral particle it may form part of a conformational epitope but when presented by rE1E2 this conformation is disrupted. These regions were also recognized by serum from vaccinated chimpanzees (Ch1587 and Ch1601) and in this context antibodies that recognize 632–667 also do not appear to be involved in neutralization (Fig. 5A).

Using specific peptide blocking we identified three new epitopes important for neutralization of HCV; aa264–318, aa448–483 and aa496–515. The epitopes at aa264–318 and aa448–483 are poorly conserved between the different HCVcc used in our study (Table 1). Epitope 264–318 has been shown to be recognized by sera from HCV-infected patients [37] and forms part of a conformational epitope recognized by a human mAb [38]. The region aa448–483 overlaps with the previously described HVR2 region and is adjacent to a putative CD81-binding domain [39]. Involvement in neutralization has not been previously demonstrated for either of these regions. Region aa496–515 is highly conserved. A Blast search of this region for GT1-6 using the Los Alamos HCV Database (http://hcv.lanl.gov) and the H77 sequence ^{496}IVPAKSVCGPVYCFTPSPVV^{515} revealed only a few isolates with

substitutions within aa502–515 out of more than 800 sequences retrieved. Further analysis of this epitope is still required to determine the mechanism of neutralization, pre or post-binding, and whether this forms part of a conformational epitope. The chimpanzee data suggests that the antibody recognizing aa496–515 also recognizes part of E1 (aa360–387). However, the VV-AB and SIN-AB preparations that also contained neutralizing antibody activity targeting the 496–515 region did not recognize the aa360–387 region (Fig. 1). The epitope aa496–515 may form part of a conformational epitope that includes part of the E1 region or the affinity purified antibody may exhibit polyreactivity as has been described for an anti-p24 monoclonal antibody [40]. Analysis of the side chain properties and predicted charge of the peptides did not identify similarities that fully account for the cross reactivity. Both peptides have a number of valine residues and each has one lysine residue. There have been a number of reports describing antibodies that show promiscuous recognition of regions sharing little or no amino acid identity [41]. Our epitope mapping data did not indicate any specific residues that were essential for binding of AB-496 to the aa496–515 region which may also help to explain the poly reactivity. We show that the lysine residue at position 500 is important, although not essential, for binding. The lysine residue in the E1 peptide sequence may also contribute to the cross reactivity. Further studies using residue substitution and random peptide phage mapping will help to establish the key binding residues in both the E1 and E2 regions and provide a better understanding of the AB-496 reactivity.

The 496–515 epitope is located between two regions proposed as CD81 binding domains [35,39]. Although from published data residues 496–512 do not appear to be directly involved in CD81 binding it can be speculated that this region is important for stability or presentation of adjacent binding regions or that antibodies binding to this region exert stearic hindrance inhibiting CD81 binding. More recently an analysis of the proposed tertiary organization of E2 identified the region from aa502 to 520 as a strong candidate for the HCV fusion loop [42].

This data is particularly encouraging in terms of vaccine development as antibodies to this epitope were induced in 2/2 chimpanzees vaccinated with rE1E2. Antibodies are also induced at low levels during natural infection in some (11%) chronically infected patients. Weak or absent immune responses to cross-neutralizing epitopes during primary infections could contribute to persistence of HCV through immune escape. Vaccines that induce cross-reactive rather than type-specific antibodies could be highly effective at preventing replication of multiple HCV GTs. Similarly, although therapeutic treatment of hepatitis B virus-infected transplant patients with hepatitis B immunoglobulin has proved successful at preventing liver reinfection, HCV immunoglobulin has not been successful when tried under similar circumstances [43]. Potentially, a mAb could be developed against this 496–515 epitope which could be combined with other cross reactive mAbs for a successful therapeutic treatment regimen in transplant patients.

Analysis of VV-AB showed that the degree of cross-neutralization conferred by antibodies to different determinants directly correlated with the degree of conservation in our HCVcc (Table 1). Overall these studies suggest that the conservation of an epitope sequence by >80% may lead to cross-neutralization although additional studies would be required to confirm this. In our studies blocking antibodies to HVR1 and 448–483 reduced the neutralization of 1a/2a virus, confirming these as neutralization epitopes, but did not affect neutralization of 1b/2a or J6/JFH1 viruses where there is low homology (Table 1). The region of aa412–419 (EPI) is known to be highly conserved between GTs; a human mAb (AP33) has been isolated to this epitope and shown to be broadly neutralizing [19,20]. Interestingly, blocking antibodies to this region had a greater impact on neutralization of J6/JFH1 and 1b/2a, probably because antibodies to this epitope contributed more to the cross-neutralization of these viruses than to the neutralization of the 1a virus where sequence-specific nAbs were important. It has been previously shown that antibodies to the region aa434–446 (designated EPII) [27,28] can interfere with the activity of antibodies to EPI. The Pepscan analysis (Fig. 1A) showed that EPII responses were minimal in VV-AB, end-point titre of <1:200, suggesting there was no negative effect in this preparation on the function of the EPI antibodies.

Finally, we assessed the efficiency of neutralization of antibody to aa496–515 compared to AB-412. We found both antibodies are less efficient at neutralizing more diverse viruses. We also consistently found that ~1.5-fold less AB-412 was required to neutralize the same amount of virus compared to antibody recognizing our new epitope at aa496–515. However, both of these eluates had substantially lower IC50 titres than an HVR1 eluate against the 1a/2a HCVcc where more than 3× as much IgG was required to neutralized the same amount of virus.

Further investigations of appropriate vaccine antigens for efficient presentation of epitopes for nAb induction are still required. It is possible that the most effective antigens for the induction of HCV nAb will not be folded in a manner that resembles HCV particles but will still be efficient at inducing cross-nAbs. Our data provides important new targets for cross protective prophylactic vaccine design and for therapeutic treatment of infected patients.

Acknowledgements

We would like to thank Dr. Charles Rice for providing J6/JFH1 cDNA and Dr. Takaji Wakita for providing JFH1 cDNA. This work was supported by internal funding from the Food and Drug Administration and by grants from the Biotechnology Engagement Program (BTEP) (BTEP#116-ISTC#3255) and the National Vaccine Program.

Appendix A. Supplementary data

Supplementary data associated with this article can be found, in the online version, at doi:10.1016/j.vaccine.2011.10.045.

References

[1] Alter MJ, Kruszon-Moran D, Nainan OV, McQuillan GM, Gao F, Moyer LA, et al. The prevalence of hepatitis C virus infection in the United States, 1988 through 1994. N Engl J Med 1999;341(August (8)):556–62.
[2] Fried MW, Shiffman ML, Reddy KR, Smith C, Marinos G, Goncales Jr FL, et al. Peginterferon alfa-2a plus ribavirin for chronic hepatitis C virus infection. N Engl J Med 2002;347(September (13)):975–82.
[3] CDC. Estimates of disease burden from viral hepatitis. Atlanta, GA: US Department of Health and Human Services, CDC; 2007. Available at http://www cdc gov/hepatitis/PDFs/disease_burden pdf.
[4] Farci P, Shimoda A, Coiana A, Diaz G, Peddis G, Melpolder JC, et al. The outcome of acute hepatitis C predicted by the evolution of the viral quasispecies. Science 2000;288(April (5464)):339–44.
[5] Erickson AL, Kimura Y, Igarashi S, Eichelberger J, Houghton M, Sidney J, et al. The outcome of hepatitis C virus infection is predicted by escape mutations in epitopes targeted by cytotoxic T lymphocytes. Immunity 2001;15(6):883–95.
[6] Ward S, Lauer G, Isba R, Walker B, Klenerman P. Cellular immune responses against hepatitis C virus: the evidence base 2002. Clin Exp Immunol 2002;128(May (2)):195–203.
[7] Simmonds P, Bukh J, Combet C, Deleage G, Enomoto N, Feinstone S, et al. Consensus proposals for a unified system of nomenclature of hepatitis C virus genotypes. Hepatology 2005;42(October (4)):962–73.
[8] Logvinoff C, Major ME, Oldach D, Heyward S, Talal A, Balfe P, et al. Neutralizing antibody response during acute and chronic hepatitis C virus infection. Proc Natl Acad Sci U S A 2004;101(July (27)):10149–54.
[9] Pestka JM, Zeisel MB, Blaser E, Schurmann P, Bartosch B, Cosset FL, et al. Rapid induction of virus-neutralizing antibodies and viral clearance in a single-source outbreak of hepatitis C. Proc Natl Acad Sci U S A 2007;104(April (14)):6025–30.
[10] Dowd KA, Netski DM, Wang XH, Cox AL, Ray SC. Selection pressure from neutralizing antibodies drives sequence evolution during acute infection with hepatitis C virus. Gastroenterology 2009;136(June (7)):2377–86.
[11] Meunier JC, Engle RE, Faulk K, Zhao M, Bartosch B, Alter H, et al. Evidence for cross-genotype neutralization of hepatitis C virus pseudo-particles and

enhancement of infectivity by apolipoprotein C1. Proc Natl Acad Sci U S A 2005;102(March (12)):4560–5.
[12] Krawczynski K, Alter MJ, Tankersley DL, Beach M, Robertson BH, Lambert S, et al. Effect of immune globulin on the prevention of experimental hepatitis C virus infection. J Infect Dis 1996;173(April (4)):822–8.
[13] Yu MY, Bartosch B, Zhang P, Guo ZP, Renzi PM, Shen LM, et al. Neutralizing antibodies to hepatitis C virus (HCV) in immune globulins derived from anti-HCV-positive plasma. Proc Natl Acad Sci U S A 2004;101(May (20)):7705–10.
[14] Houghton M, Abrignani S. Prospects for a vaccine against the hepatitis C virus. Nature 2005;436(August (7053)):961–6.
[15] Bartosch B, Dubuisson J, Cosset FL. Infectious hepatitis C virus pseudo-particles containing functional E1–E2 envelope protein complexes. J Exp Med 2003;197(March (5)):633–42.
[16] Hsu M, Zhang J, Flint M, Logvinoff C, Cheng-Mayer C, Rice CM, et al. Hepatitis C virus glycoproteins mediate pH-dependent cell entry of pseudotyped retroviral particles. Proc Natl Acad Sci U S A 2003;100(June (12)):7271–6.
[17] Wakita T, Pietschmann T, Kato T, Date T, Miyamoto M, Zhao Z, et al. Production of infectious hepatitis C virus in tissue culture from a cloned viral genome. Nat Med 2005;11(July (7)):791–6.
[18] Lindenbach BD, Evans MJ, Syder AJ, Wolk B, Tellinghuisen TL, Liu CC, et al. Complete replication of hepatitis C virus in cell culture. Science 2005;309(July (5734)):623–6.
[19] Owsianka A, Tarr AW, Juttla VS, Lavillette D, Bartosch B, Cosset FL, et al. Monoclonal antibody AP33 defines a broadly neutralizing epitope on the hepatitis C virus E2 envelope glycoprotein. J Virol 2005;79(September (17)):11095–104.
[20] Tarr AW, Owsianka AM, Timms JM, McClure CP, Brown RJ, Hickling TP, et al. Characterization of the hepatitis C virus E2 epitope defined by the broadly neutralizing monoclonal antibody AP33. Hepatology 2006;43(March (3)):592–601.
[21] Law M, Maruyama T, Lewis J, Giang E, Tarr AW, Stamataki Z, et al. Broadly neutralizing antibodies protect against hepatitis C virus quasispecies challenge. Nat Med 2008;14(January (1)):25–7.
[22] Major ME, Mihalik K, Fernandez J, Seidman J, Kleiner D, Kolykhalov AA, et al. Long-term follow-up of chimpanzees inoculated with the first infectious clone for hepatitis C virus. J Virol 1999;73(April (4)):3317–25.
[23] Puig M, Major ME, Mihalik K, Yu MY, Feinstone SM. Immunization of chimpanzees with an envelope protein-based vaccine enhances specific humoral and cellular immune responses that delay hepatitis C virus infection. Vaccine 2004;22:991–1000.
[24] Dubuisson J, Hsu HH, Cheung RC, Greenberg HB, Russell DG, Rice CM. Formation and intracellular localization of hepatitis C virus envelope glycoprotein complexes expressed by recombinant vaccinia and Sindbis viruses. J Virol 1994;68:6147–60.
[25] Reed LJ, Muench H. A simple method of estimating fifty per cent endpoints. Am J Hyg 1938;27(3):493–7.
[26] Blight KJ, McKeating JA, Rice CM. Highly permissive cell lines for subgenomic and genomic hepatitis C virus RNA replication. J Virol 2002;76(December (24)):13001–14.
[27] Zhang P, Zhong L, Struble EB, Watanabe H, Kachko A, Mihalik K, et al. Depletion of interfering antibodies in chronic hepatitis C patients and vaccinated chimpanzees reveals broad cross-genotype neutralizing activity. Proc Natl Acad Sci U S A 2009;106(May (18)):7537–41.
[28] Zhang P, Wu CG, Mihalik K, Virata-Theimer ML, Yu MY, Alter HJ, et al. Hepatitis C virus epitope-specific neutralizing antibodies in Igs prepared from human plasma. Proc Natl Acad Sci U S A 2007;104(May (20)):8449–54.
[29] Major ME, Dahari H, Mihalik K, Puig M, Rice CM, Neumann AU, et al. Hepatitis C virus kinetics and host responses associated with disease and outcome of infection in chimpanzees. Hepatology 2004;39(June (6)):1709–20.
[30] Johansson DX, Voisset C, Tarr AW, Aung M, Ball JK, Dubuisson J, et al. Human combinatorial libraries yield rare antibodies that broadly neutralize hepatitis C virus. Proc Natl Acad Sci U S A 2007;104(October (41)):16269–74.
[31] Elmowalid GA, Qiao M, Jeong SH, Borg BB, Baumert TF, Sapp RK, et al. Immunization with hepatitis C virus-like particles results in control of hepatitis C virus infection in chimpanzees. Proc Natl Acad Sci U S A 2007;104(May (20)):8427–32.
[32] Li Y, Cleveland B, Klots I, Travis B, Richardson BA, Anderson D, et al. Removal of a single N-linked glycan in human immunodeficiency virus type 1 gp120 results in an enhanced ability to induce neutralizing antibody responses. J Virol 2008;82(January (2)):638–51.
[33] Brinster C, Muguet S, Lone YC, Boucreux D, Renard N, Fournillier A, et al. Different hepatitis C virus nonstructural protein 3 (Ns3)-DNA-expressing vaccines induce in HLA-A2.1 transgenic mice stable cytotoxic T lymphocytes that target one major epitope. Hepatology 2001;34(6):1206–17.
[34] Triyatni M, Vergalla J, Davis AR, Hadlock KG, Foung SK, Liang TJ. Structural features of envelope proteins on hepatitis C virus-like particles as determined by anti-envelope monoclonal antibodies and CD81 binding. Virology 2002;298(June (1)):124–32.
[35] Owsianka A, Clayton RF, Loomis-Price LD, McKeating JA, Patel AH. Functional analysis of hepatitis C virus E2 glycoproteins and virus-like particles reveals structural dissimilarities between different forms of E2. J Gen Virol 2001;82(August (Pt 8)):1877–83.
[36] Owsianka AM, Timms JM, Tarr AW, Brown RJ, Hickling TP, Szwejk A, et al. Identification of conserved residues in the E2 envelope glycoprotein of the hepatitis C virus that are critical for CD81 binding. J Virol 2006;80(September (17)):8695–704.
[37] Zibert A, Kraas W, Ross RS, Meisel H, Lechner S, Jung G, et al. Immunodominant B-cell domains of hepatitis C virus envelope proteins E1 and E2 identified during early and late time points of infection. J Hepatol 1999;30(February (2)):177–84.
[38] Petit MA, Jolivet-Reynaud C, Peronnet E, Michal Y, Trepo C. Mapping of a conformational epitope shared between E1 and E2 on the serum-derived human hepatitis C virus envelope. J Biol Chem 2003;278(November (45)):44385–92.
[39] Flint M, Maidens C, Loomis-Price LD, Shotton C, Dubuisson J, Monk P, et al. Characterization of hepatitis C virus E2 glycoprotein interaction with a putative cellular receptor, CD81. J Virol 1999;73(August (8)):6235–44.
[40] Winkler K, Kramer A, Kuttner G, Seifert M, Scholz C, Wessner H, et al. Changing the antigen binding specificity by single point mutations of an anti-p24 (HIV-1) antibody. J Immunol 2000;165(October (8)):4505–14.
[41] Marchalonis JJ, Adelman MK, Robey IF, Schluter SF, Edmundson AB. Exquisite specificity and peptide epitope recognition promiscuity, properties shared by antibodies from sharks to humans. J Mol Recognit 2001;14(March (2)):110–21.
[42] Krey T, d'Alayer J, Kikuti CM, Saulnier A, Damier-Piolle L, Petitpas I, et al. The disulfide bonds in glycoprotein E2 of hepatitis C virus reveal the tertiary organization of the molecule. PLoS Pathog 2010;6(February (2)):e1000762.
[43] Davis GL, Nelson DR, Terrault N, Pruett TL, Schiano TD, Fletcher CV, et al. A randomized, open-label study to evaluate the safety and pharmacokinetics of human hepatitis C immune globulin (Civacir) in liver transplant recipients. Liver Transpl 2005;11(August (8)):941–9.

Research Article

EASL EUROPEAN ASSOCIATION FOR THE STUDY OF THE LIVER | JOURNAL OF HEPATOLOGY

Serum metabolomics reveals γ-glutamyl dipeptides as biomarkers for discrimination among different forms of liver disease

Tomoyoshi Soga[1,*], Masahiro Sugimoto[1], Masashi Honma[2], Masayo Mori[1], Kaori Igarashi[1], Kasumi Kashikura[1], Satsuki Ikeda[1], Akiyoshi Hirayama[1], Takehito Yamamoto[2], Haruhiko Yoshida[3], Motoyuki Otsuka[3], Shoji Tsuji[4], Yutaka Yatomi[4], Tadayuki Sakuragawa[5], Hisayoshi Watanabe[6], Kouei Nihei[7], Takafumi Saito[6], Sumio Kawata[6], Hiroshi Suzuki[2], Masaru Tomita[1], Makoto Suematsu[5]

[1]*Institute for Advanced Biosciences, Keio University, Tsuruoka 997-0052, Japan;* [2]*Department of Pharmacy, The University of Tokyo Hospital, Hongo, Bunkyo-ku, Tokyo 113-8655, Japan;* [3]*Department of Gastroenterology, Faculty of Medicine, The University of Tokyo, Hongo, Bunkyo-ku, Tokyo 113-8655, Japan;* [4]*Department of Neurology, Division of Neuroscience, Graduate School of Medicine, The University of Tokyo, Hongo, Bunkyo-ku, Tokyo 113-8655, Japan;* [5]*Department of Biochemistry, JST ERATO Suematsu Gas Biology Project, School of Medicine, Keio University, Shinanomachi, Shinjuku-ku, Tokyo 160-8582, Japan;* [6]*Department of Gastroenterology, Yamagata University School of Medicine, Yamagata 990-9585, Japan;* [7]*Department of Surgery, Shonai Hospital, 4-20 Izumi-cho, Tsuruoka 997-8515, Japan*

Background & Aims: We applied a metabolome profiling approach to serum samples obtained from patients with different liver diseases, to discover noninvasive and reliable biomarkers for rapid-screening diagnosis of liver diseases.

Methods: Using capillary electrophoresis and liquid chromatography mass spectrometry, we analyzed low molecular weight metabolites in a total of 248 serum samples obtained from patients with nine types of liver disease and healthy controls.

Results: We found that γ-glutamyl dipeptides, which were biosynthesized through a reaction with γ-glutamylcysteine synthetase, were indicative of the production of reduced glutathione, and that measurement of their levels could distinguish among different liver diseases. Multiple logistic regression models facilitated the discrimination between specific and other liver diseases and yielded high areas under receiver-operating characteristic curves. The area under the curve values in training and independent validation data were 0.952 and 0.967 in healthy controls, 0.817 and 0.849 in drug-induced liver injury, 0.754 and 0.763 in asymptomatic hepatitis B virus infection, 0.820 and 0.762 in chronic hepatitis B, 0.972 and 0.895 in hepatitis C with persistently normal alanine transaminase, 0.917 and 0.707 in chronic hepatitis C, 0.803 and 0.993 in cirrhosis type C, and 0.762 and 0.803 in hepatocellular carcinoma, respectively. Several γ-glutamyl dipeptides also manifested potential for differentiating between nonalcoholic steatohepatitis and simple steatosis.

Conclusions: γ-Glutamyl dipeptides are novel biomarkers for liver diseases, and varying levels of individual or groups of these peptides have the power to discriminate among different forms of hepatic disease.

Keywords: γ-Glutamyl dipeptides; Metabolomics; Biomarker; Capillary electrophoresis mass spectrometry; Oxidative stress; Glutathione; Hepatocellular carcinoma; Nonalcoholic steatohepatitis; Hepatitis C virus.

Received 15 July 2010; received in revised form 17 January 2011; accepted 24 January 2011; available online 18 February 2011

* Corresponding author. Address: Institute for Advanced Biosciences, Keio University, 246-2 Mizukami, Kakuganji, Tsuruoka, Yamagata 997-0052, Japan. Tel.: +81 235 29 0528; fax: +81 0235 29 0574.

E-mail address: soga@sfc.keio.ac.jp (T. Soga).

Abbreviations: HCC, hepatocellular carcinoma; AST, aspartate transaminase; ALT, alanine transaminase; γ-GTP, γ-glutamyl transpeptidase; CT, computed tomography; NAFLD, nonalcoholic fatty liver disease; SS, simple steatosis; NASH, nonalcoholic steatohepatitis; CE-TOFMS, capillary electrophoresis time-of-flight mass spectrometry; GSH, reduced glutathione; GC, gastric cancer; GCS, γ-glutamylcysteine synthetase; C, healthy control; DI, drug-induced liver injury; AHB, asymptomatic hepatitis B virus infection; CHB, chronic hepatitis B; CNALT, hepatitis C with persistently normal alanine transaminase; CHC, chronic hepatitis C; CIR, cirrhosis type C; HBs, hepatitis B surface; HBV, hepatitis B virus; HCV, hepatitis C virus; AFP, α-fetoprotein; PIVKA, protein induced by vitamin K antagonist; LC–MS/MS, liquid chromatography–electrospray tandem mass spectrometry; MLR, multiple logistic regression; APAP, acetaminophen; GS, glutathione synthetase; BSO, buthionine sulfoximine; DEM, diethylmaleate; ROS, reactive oxygen species.

Introduction

Acute or chronic viral hepatitis affects populations around the world, and the disease often progresses from chronic hepatitis and cirrhosis to hepatocellular carcinoma (HCC) [1]. Accurate diagnosis at earlier stages is necessary for improved therapeutic outcome. However, the diagnostic procedures are laborious and not risk-free. Patients with suspected liver damage are initially subjected to liver function tests that include the assessment of aspartate transaminase (AST), alanine transaminase (ALT), and γ-glutamyl transpeptidase (γ-GTP) serum levels. If these levels are abnormal, patients are then subjected to diagnostic imaging, such as ultrasound and computed tomography (CT), and assays to determine the presence of antibodies against hepatitis virus. Finally, a liver biopsy may be recommended to evaluate the severity of inflammation or fibrosis and to confirm the indications for antiviral therapy.

Recently, nonalcoholic fatty liver disease (NAFLD) has become the most common liver disease in western countries. It

encompasses a wide spectrum of conditions associated with over-accumulation of fat in the liver, ranging from simple steatosis (SS) to nonalcoholic steatohepatitis (NASH), and cirrhosis [2]. Although SS typically follows a benign non-progressive clinical course, NASH may eventually develop into cirrhosis and HCC. To date, a liver biopsy remains the gold standard for the diagnosis of NASH [3]. However, since the biopsy procedures carry the risk of mortality [4,5], the noninvasive identification of biomarkers, that can provide reliable differential diagnoses for the characterization of liver diseases, is desirable.

Metabolomics, which can be defined as measurement of the levels of all cellular metabolites, has emerged as a powerful new tool for discovering new low molecular weight biomarkers. Its utility has been demonstrated by the identification of new biomarkers for prostate cancer [6], Parkinson's disease [7], type 2 diabetes mellitus [8], acute myocardial ischemia [9], and pre-eclampsia [10].

Recently, we developed new metabolomic profiling approaches based on capillary electrophoresis mass spectrometry [11] and capillary electrophoresis–time-of-flight mass spectrometry (CE–TOFMS) [12–14]. The efficacy of CE–TOFMS was demonstrated by the discovery of ophthalmate (γ-glutamyl-2-aminobutyrylglycine) as a biomarker; in mice, reduced glutathione (GSH) depletion produced acetaminophen-induced hepatotoxicity [12,14]. In this study, to discover new noninvasive biomarkers for human liver diseases, we comprehensively analyzed the serum metabolites in a total of 248 samples from patients with nine types of liver disease or gastric cancer (GC) and from normal individuals using our metabolomic approaches, and found increased levels of γ-glutamyl dipeptides in the majority of the liver diseases. Moreover, we found that γ-glutamyl dipeptides were synthesized via the ligation of glutamate with various amino acids and amines by the γ-glutamylcysteine synthetase (GCS), an enzyme that is feedback-inhibited by GSH, and that the levels of γ-glutamyl dipeptides were indicative of the amount of GSH production. The concentrations of serum γ-glutamyl dipeptides varied with the stage and type of liver disease and can, therefore, act as new biomarkers for liver diseases. Here, we report that a highly specific set of γ-glutamyl dipeptides, alone or in combination with transaminases and methionine sulfoxide, can effectively distinguish specific liver diseases from other hepatic injuries and healthy control samples.

Materials and methods

Serum samples

A total of 248 serum samples were obtained from three institutes, Yamagata University Hospital (YUH; Yamagata, Japan), University of Tokyo Hospital (UTH; Tokyo, Japan) and Shonai Hospital (SH; Tsuruoka, Japan). The 162 YUH cases comprised 53 healthy controls (C) and patients with drug-induced liver injury (DI; $n = 10$), asymptomatic hepatitis B virus infection (AHB; $n = 9$), chronic hepatitis B (CHB; $n = 7$), hepatitis C with persistently normal alanine transaminase (CNALT; $n = 10$), chronic hepatitis C (CHC; $n = 24$), cirrhosis type C (CIR; $n = 10$), HCC ($n = 19$), SS ($n = 9$) and NASH ($n = 11$). The 75 UTH cases comprised four controls and patients with DI ($n = 17$), AHB ($n = 7$), CHB ($n = 7$), CNALT ($n = 8$), CHC ($n = 11$), CIR ($n = 8$) and HCC ($n = 13$). The 11 SH cases were all GC patients. Written informed consent was obtained from all the participants and the study protocol conformed to the ethical guidelines of the 1975 Declaration of Helsinki as reflected in a priori approval by the appropriate institutional review boards of YUH, UTH, and SH. The study subjects were patients with viral liver diseases, drug-induced hepatotoxicity or NAFLD who were referred to the Department of Gastroenterology and Hepatology at YUH, UTH, or SH.

Clinical diagnosis

All the healthy controls had normal liver function and no viral hepatitis infection, and none were alcoholics. The AHB and CNALT patients were confirmed to have normal liver function and to be positive for hepatitis B surface (HBs) antigen and hepatitis B virus (HBV) DNA, or for anti-hepatitis C virus (HCV) antibodies and HCV RNA, respectively. DI was diagnosed based on abnormal values on biochemical tests, absence of other hepatic diseases, and a history of treatment with drugs suspected of being probable causes of DI. The suspected medications were different, and the biochemical test results in each patient normalized after their withdrawal.

CHC and CIR were diagnosed on the basis of physical examination, biochemical tests, ultrasonography, and CT findings. Some patients with chronic hepatitis provided informed consent for a liver biopsy, and the procedure was performed to confirm the accuracy of the diagnosis. The diagnosis of CHB and CHC was based on increased ALT levels (above the upper limit of the normal range) in at least two blood samples assayed over a 6-month period, and the presence of detectable HBs antigen and HBV DNA or detectable anti-HCV antibodies and HCV RNA, respectively. HCV infection was causative in all cirrhosis patients, and they manifested symptoms of portal hypertension, such as splenomegaly, esophageal varices, encephalopathy, or ascites.

The diagnosis of HCC was based on ultrasonography, CT, and MRI findings that revealed features typical of HCC. HCV was causative in all cases, and the α-fetoprotein (AFP) and protein induced by vitamin K antagonist (PIVKA)-II levels were assayed in all HCC patients.

All of the SS and NASH patients underwent liver biopsy. The tissue samples were stained with hematoxylin–eosin, reticulin, and Masson trichrome; and examined by the same experienced pathologist who was blinded to the clinical data. The histological criterion for the diagnosis of NAFLD was the presence of fatty changes in hepatocytes. When hepatocytes exhibited macrovesicular steatosis, the differential diagnosis was SS or NASH. The criteria for a diagnosis of steatohepatitis were the presence of lobular inflammation and either ballooning cells or perisinusoidal/pericellular fibrosis, in addition to steatosis in the liver specimen. No patient with autoimmune hepatitis, primary biliary cirrhosis, sclerosing cholangitis, hemochromatosis, α1-antitrypsin deficiency, Wilson's disease, or alcoholic liver injury was included. All patients with GC were diagnosed by pathologic studies of biopsy tissues.

Analytical and statistical technologies for biomarker discovery

Using a total of 237 samples from YUH (training cohort, $n = 162$) and UTH (validation cohort, $n = 75$) (Table 1), we performed CE–TOFMS for a comprehensive analysis of the metabolite changes to discover new biomarkers in the diagnosis of human liver diseases. To facilitate peak identification and quantification, we analyzed 162 metabolic standards listed in the KEGG LIGAND database [15] before analyzing the samples. Global mass scanning over a 50–1000 m/z range was applied in the CE–TOFMS mode [12]. To focus on γ-glutamyl peptides, we employed a highly sensitive method using liquid chromatography electrospray tandem mass spectrometry (LC–MS/MS) with multiple reactions monitoring for analyses of the patient serum samples. The Kruskal–Wallis test and Dunn's post-test were used to assess the statistical significance of differences among C, DI, AHB, CHB, CNALT, CHC, CIR, and HCC. The Mann–Whitney test was used to evaluate the statistical significance of differences between SS and NASH. The algorithm of the feature selection for the multiple logistic regression (MLR) models is described in the Supplementary data.

Results

Discovery of γ-glutamyl dipeptides in serum by metabolomic profiling

The CE–TOFMS analysis quantified the levels of 49 metabolites in the serum samples (Supplementary Tables 1 and 2) and revealed increases in many compounds in most liver diseases. We identified these compounds as γ-glutamyl dipeptides (e.g., γ-Glu-Gly, γ-Glu-Ala, γ-Glu-Ser, γ-Glu-Val, γ-Glu-Thr, γ-Glu-Taurine, γ-Glu-Leu, γ-Glu-Gln, γ-Glu-Lys, γ-Glu-Glu, γ-Glu-Met, γ-Glu-His, γ-Glu-Phe, γ-Glu-Arg, γ-Glu-Citrulline, γ-Glu-Tyr, and γ-Glu-Trp) by comparing their migration times and exact molecular

Table 1. Summary of patient information.

Clinical information		Training cohort (n = 162)	Defect no.	Validation cohort (n = 75)	Defect no.	*p* value
Age (years)						
	Median	61	0	66	0	0.47
	Interquartile range	51-73	0	55-70	0	
Sex (n)	Male	73	0	52	0	0.0007*
	Female	89	0	23	0	
AST (UL^{-1})						
	C	21.5 ± 5.40	0	25.3 ± 3.60	0	0.074
	DI	274 ± 567	0	81.2 ± 84.9	0	0.15
	AHB	25.0 ± 6.81	2	23.9 ± 6.90	0	0.71
	CHB	109 ± 164	0	150 ± 146	0	0.0059
	CNALT	24.1 ± 3.80	0	23.8 ± 6.00	0	0.72
	CHC	62.8 ± 65.3	0	110 ± 51.0	0	0.0010
	CIR	54.6 ± 27.1	0	58.0 ± 26.1	0	0.69
	HCC	71.3 ± 52.8	0	35.0 ± 24.5	0	0.0010
	SS	41.2 ± 11.5	0			
	NASH	78.6 ± 48.0	0			
ALT (UL^{-1})						
	C	17.7 ± 4.70	0	25.0 ± 8.30	0	0.062
	DI	253 ± 343	0	115 ± 132	0	0.15
	AHB	26.6 ± 18.6	2	23.1 ± 5.60	0	0.40
	CHB	117 ± 162	0	173 ± 131	0	0.0060
	CNALT	17.9 ± 4.10	0	21.5 ± 3.60	0	0.074
	CHC	79.4 ± 81.0	0	160 ± 116	0	0.0036
	CIR	40.7 ± 21.9	0	57.3 ± 42.4	0	0.69
	HCC	57.9 ± 58.8	0	25.0 ± 21.6	0	0.0026
	SS	72.2 ± 24.5	0			
	NASH	121 ± 140	0			
γ-GTP						
	C	20.7 ± 8.60	0	—	4	—
	DI	190 ± 236	0	46.2 ± 29.5	5	0.010
	AHB	31.1 ± 24.1	2	—	7	—
	CHB	52.8 ± 38.1	1	—	7	—
	CNALT	150 ± 5.70	0	—	8	—
	CHC	48.5 ± 36.4	0	—	11	—
	CIR	28.8 ± 17.9	0	49.6 ± 53.1	0	0.17
	HCC	51.2 ± 31.1	0	—	13	—
	SS	61.8 ± 43.7	0			
	NASH	98.7 ± 99.1	0			
AFP						
	CHC	6.40 ± 7.40	3	—	11	—
	CIR	35.1 ± 71.8	0	14 ± 15.6	0	0.63
	HCC	9.79×10^2 ± 1.73×10^3	0	7.04×10^3 ± 2.52×10^4	0	0.024
PIVKA-II						
	HCC	1.57×10^2 ± 1.87×10^2	0	7.78×10^3 ± 2.77×10^4	0	0.022

*Chi-square test. The others *p* values were obtained by the Mann–Whitney *U*-test.

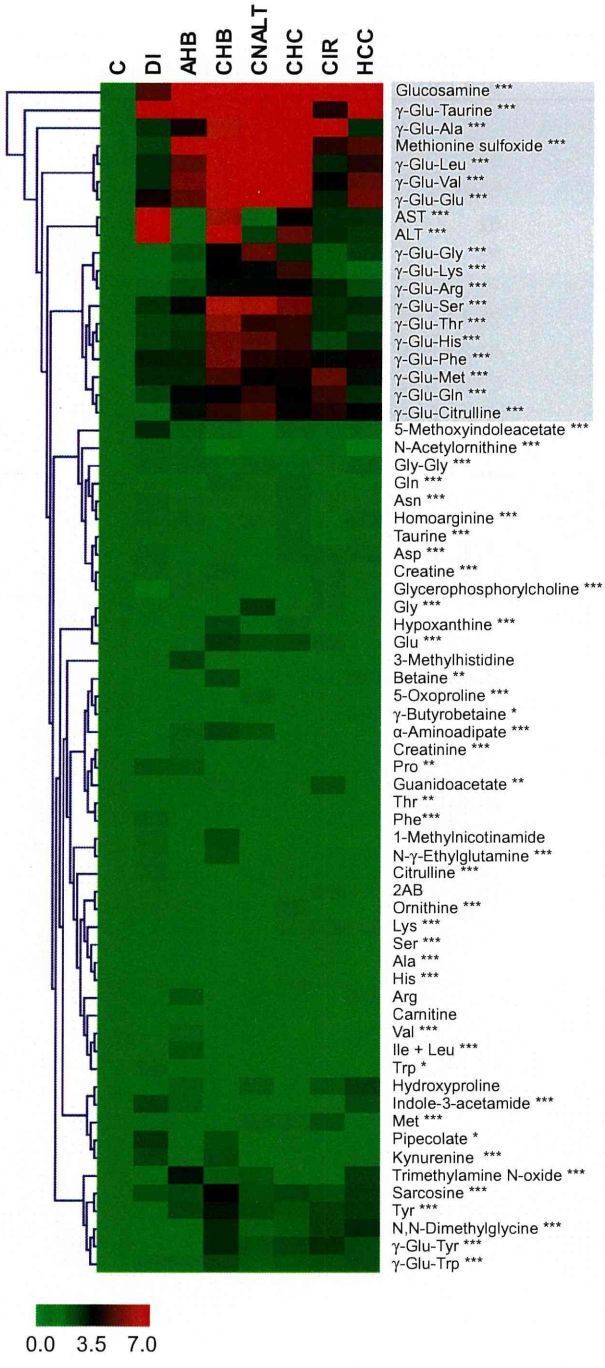

Fig. 1. Heat map representing the hierarchical clustering of 67 compounds in serum samples from controls and patients with various types of liver disease in both cohorts. Each row shows data for a specific metabolite or transaminase, and each column shows data for the healthy controls and patients with liver diseases. The compound concentration in each individual was divided by the average concentration in the healthy controls and the obtained values were then averaged again for each disease. The metabolites highlighted in blue showed large fold changes (disease/control ratios of >2.5) in an average of seven liver diseases. $^{*}p$ <0.05, $^{**}p$ <0.01, $^{***}p$ <0.0001, significance difference by the Kruskal–Wallis test. The compounds were clustered based on elucidation distances. Red and green denote relatively high and low concentrations, respectively, compared with the average concentration.

weights with those of the standards. Significant differences were observed among controls and liver diseases (p <0.0001; Kruskal–Wallis test) except for γ-Glu-Met in the validation data (Supplementary Tables 1 and 2). Correlational cluster analyses of 67 compounds showed that all the γ-glutamyl dipeptides except for γ-Glu-Tyr and γ-Glu-Trp were clustered with AST, ALT, and metabolites involved in oxidative stress responses, namely glucosamine [16] and methionine sulfoxide [17–19] (Fig. 1).

Statistical analysis and validation for biomarker discovery

From the serum samples obtained at YUH, we selected 89 liver disease patients including DI, AHB, CHB, CNALT, CHC, CIR, and HCC patients, and 53 healthy controls with no significant differences in the age distribution between the training and validation cohorts (Table 1). As shown in the whisker box plots for the training cohort (Fig. 2), the levels of γ-glutamyl dipeptides and of AST and ALT, as commonly used hepatocyte biomarkers, were increased in different patterns in comparison with C. For example, the AST and ALT levels were significantly increased in patients with DI, CHB, CHC, CIR, and HCC (p <0.05; Dunn's post-test), but not in those with AHB and CNALT (Fig. 2). On the other hand, significant increases were observed in the levels of γ-Glu-Ser, γ-Glu-Val, γ-Glu-Thr, γ-Glu-Leu, and γ-Glu-Phe (p <0.05; Dunn's post-test) in AHB and in the levels of all the γ-glutamyl derivatives of amino acids (p <0.05; Dunn's post-test) except for ophthalmate, γ-Glu-Thr, and γ-Glu-Trp in CNALT (Fig. 2 and Supplementary Table 1). Oxidative metabolites, methionine sulfoxide, and glucosamine were significantly increased in all diseases (p <0.05; Dunn's post-test) and in CHB, CNALT, and CHC (p <0.0001; Dunn's post-test), respectively (Fig. 2).

To assess their abilities to discriminate specific liver diseases from other liver diseases, we developed MLR models using combinations of several components of the γ-glutamyl dipeptides, transaminases, and oxidative metabolites using the training dataset. For example, an MLR model incorporating four selected biomarkers (γ-Glu-Ala, γ-Glu-Citrulline, γ-Glu-Thr, and γ-Glu-Phe) was able to differentiate HCC from the other groups (C, DI, AHB, CHB, CNALT, CHC, and CIR) with an area under the receiver-operating characteristic (ROC) curve (AUC) value of 0.762 (95% CI 0.647–0.877, $p = 0.00025$). The probability (p) of HCC is calculated by: $\log(p/(1-p)) = -1.87 - 1.13 \times$ γ-Glu-Ala $+ 3.51 \times$ γ-Glu-Citrulline $- 1.65 \times$ γ-Glu-Thr $+ 6.99 \times$ γ-Glu-Phe (Table 2). When the concentrations of γ-Glu-Ala, γ-Glu-Citrulline, γ-Glu-Thr, and γ-Glu-Phe are 1.7, 0.84, 0.54, and 0.34 μM, respectively, the probability of HCC is 65.5%. All the MLR models achieved high AUC values at statistically significant levels (between 0.754 and 0.972, p <0.011) (Fig. 3, Table 2 and Supplementary Table 3).

The developed MLR models were evaluated in a blinded manner using an independent cohort (YUH) consisting of 75 individuals who were not members of the training cohort (Supplementary Table 2). We found that all of the MLR models also produced high AUC values at statistically significant levels (between 0.707 and 0.993, p <0.023) (Fig. 3, Table 2 and Supplementary Table 3). Although C, CHB, and CHC were each differentiated from the other groups by a single γ-glutamyl dipeptide (γ-Glu-Phe, γ-Glu-Thr, and γ-Glu-Lys, respectively), the MLR models for the other diseases required multiple biomarkers to achieve accurate discrimination (Table 2). The odds ratios of ALT, AST, and methionine sulfoxide were close to 1.0 compared with the odds ratios of the γ-glutamyl dipeptides, indicating their

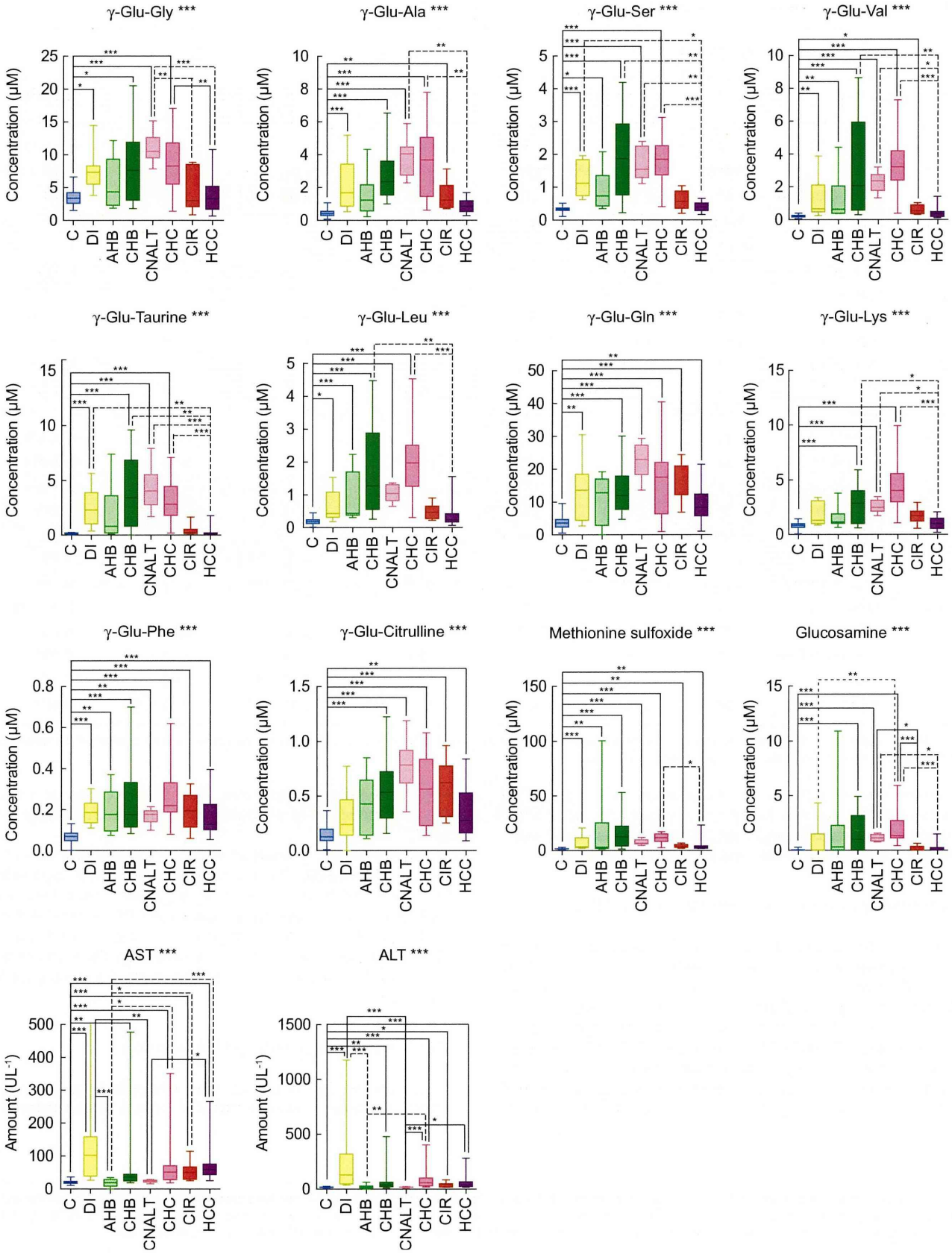
γ-Glu-Gly ***
γ-Glu-Ala ***
γ-Glu-Ser ***
γ-Glu-Val ***
γ-Glu-Taurine ***
γ-Glu-Leu ***
γ-Glu-Gln ***
γ-Glu-Lys ***
γ-Glu-Phe ***
γ-Glu-Citrulline ***
Methionine sulfoxide ***
Glucosamine ***
AST ***
ALT ***
Concentration (μM)
Amount (UL-1)
C
DI
AHB
CHB
CNALT
CHC
CIR
HCC

Table 2. Biomarkers for discriminating each liver disease selected by MLR models.

Group	Biomarker	Coefficient	95% CI		Odds ratio	95% CI		*p* value
C	(Intercept)	5.77	3.84	8.32	—	—	—	<0.0001
	γ-Glu-Phe	-58.2	-84.3	-39.0	5.16×10^{-26}	2.47×10^{-37}	1.15×10^{-17}	<0.0001
DI	(Intercept)	-3.08	-4.49	-1.94	—	—	—	<0.0001
	ALT	0.020	7.89×10^{-3}	0.034	1.02	1.01	1.03	2.00×10^{-3}
	γ-Glu-Citrulline	-1.55	-5.01	1.13	0.21	6.68×10^{-3}	3.11	0.31
AHB	(Intercept)	-1.52	-3.35	0.63	—	—	—	0.12
	AST	-0.057	-0.15	-4.96×10^{-3}	0.94	0.86	1.00	0.12
	Methionine sulfoxide	0.072	0.018	0.15	1.08	1.02	1.17	0.047
CHB	(Intercept)	-4.52	-6.33	-3.24	—	—	—	<0.0001
	γ-Glu-Thr	1.52	0.65	2.63	4.58	1.91	13.9	2.30×10^{-3}
CNALT	(Intercept)	-0.76	-3.15	1.94	—	—	—	0.55
	ALT	-0.16	-0.34	-0.049	0.85	0.71	0.95	0.032
	γ-Glu-Taurine	0.80	0.43	1.31	2.23	1.54	3.72	3.00×10^{-4}
CHC	(Intercept)	-4.73	-6.39	-3.47	—	—	—	<0.0001
	γ-Glu-Lys	1.27	0.85	1.82	3.57	2.34	6.14	<0.0001
CIR	(Intercept)	-2.79	-4.05	-1.55	—	—	—	<0.0001
	γ-Glu-Ala	1.80	0.42	3.52	6.05	1.52	33.7	0.020
	γ-Glu-Leu	-0.066	-3.06	2.24	0.94	0.047	9.42	0.96
	γ-Glu-Ser	-1.35	-5.35	1.86	0.26	4.77×10^{-3}	6.44	0.41
	γ-Glu-Taurine	-2.28	-5.07	-0.33	0.10	6.27×10^{-3}	0.72	0.064
HCC	(Intercept)	-1.87	-2.90	-0.90	—	—	—	2.00×10^{-4}
	γ-Glu-Ala	-1.13	-2.44	-0.14	0.32	0.087	0.87	0.050
	γ-Glu-Citrulline	3.51	0.45	7.00	33.4	1.57	1.10×10^{3}	0.033
	γ-Glu-Thr	-1.65	-5.12	0.49	0.19	5.95×10^{-3}	1.63	0.27
	γ-Glu-Phe	6.99	-0.52	14.7	1.09×10^{3}	5.92×10^{-1}	2.50×10^{6}	0.063

Note: The en-dashes in the 95% CI columns indicate that these values could not be calculated. Biomarker and coefficients are used in MLR model to calculate the probability of each disease. Intercept indicates the constant term in MLR models.

relatively lower contributions to the separation ability of the MLR models (Table 2). Overall, for all types of liver diseases, the MLR models mostly based on γ-glutamyl dipeptides provided complementary results, even in the second (validation) cohort.

γ-Glutamyl dipeptides as biomarkers for HCC and NAFLD

To evaluate the diagnostic potential of γ-glutamyl dipeptides for HCC, we compared their diagnostic abilities with that of AFP, an established marker for HCC (Fig. 4). We found that the MLR models using four γ-glutamyl dipeptides (γ-Glu-Ala, γ-Glu-Citrulline, γ-Glu-Thr, γ-Glu-Phe) (Table 2) were better at distinguishing HCC from CHC and CIR (AUC = 0.881) than AFP (AUC = 0.760) (Fig. 4).

We further investigated the biomarker specificities by comparing the serum γ-glutamyl dipeptide levels in GC and HCC patients (Supplementary Fig. 2 and Table 4). The analyses revealed significant differences, with the exception of γ-Glu-Phe, and the levels of γ-glutamyl dipeptides were notably low in GC.

Differences in the levels of γ-glutamyl dipeptides were also observed in NAFLD. The levels of six γ-glutamyl dipeptides (γ-Glu-Val, γ-Glu-Thr, γ-Glu-Leu, γ-Glu-His, γ-Glu-Phe, and γ-Glu-Arg) were significantly higher (p <0.05; Mann–Whitney test) in SS than in NASH (Supplementary Fig. 3 and Table 5). Although further investigations are necessary, these dipeptides can be used as noninvasive biomarkers in rapid screening for SS and NASH.

Mechanism of γ-glutamyl dipeptide biosynthesis

To confirm the γ-glutamyl dipeptide biosynthesis pathway, the hepatic metabolism was investigated using a mouse model. In

Fig. 2. Representative whisker box plots of the serum levels of detected transaminases and metabolites in the training cohort. The horizontal lines indicate the upper median, median, and lower median, and the whiskers show the maximum and minimum levels. One plot for AST was outside the range (>500 U/L). *p <0.05, **p <0.01, ***p <0.0001, significance difference by the Kruskal–Wallis test and Dunn's post-test for each marker and two groups in each marker, respectively.

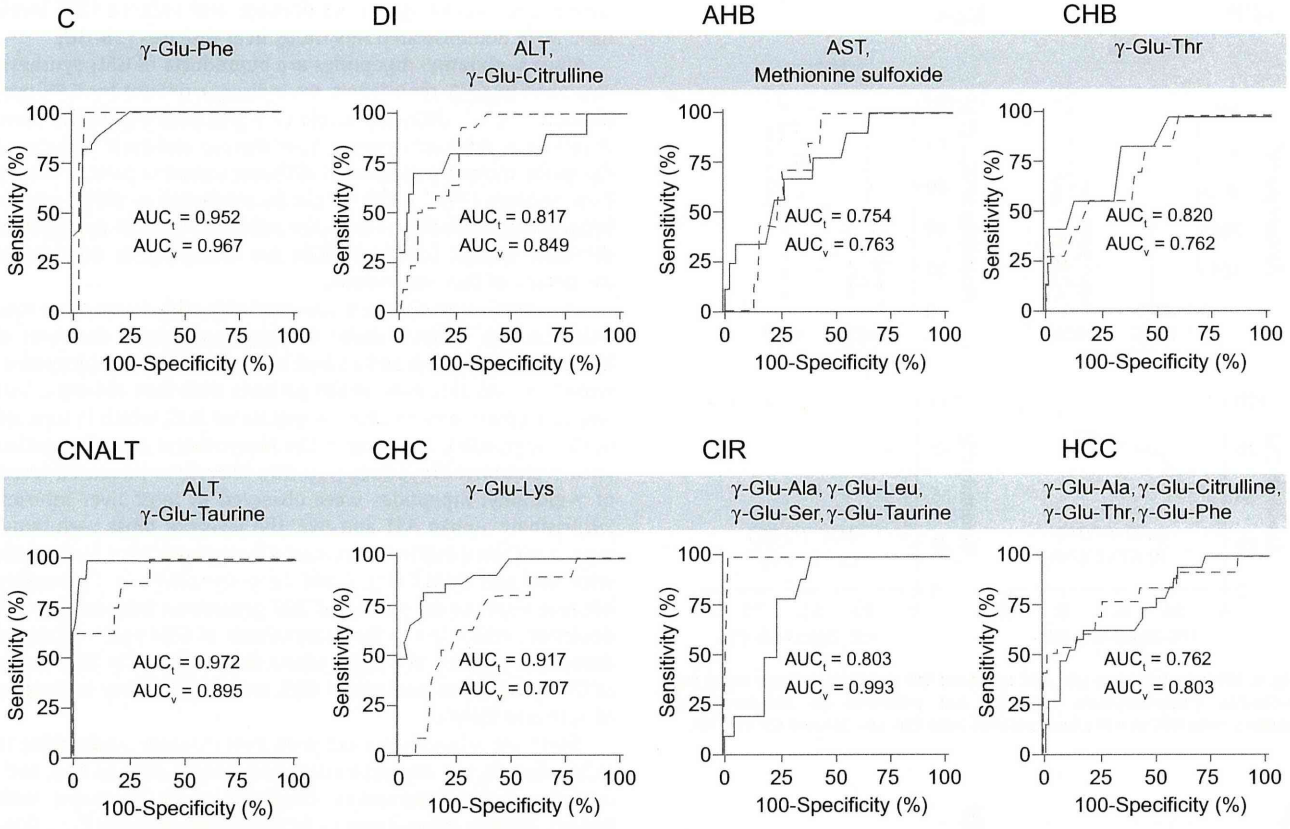

Fig. 3. ROC curve analyses of the ability of γ-glutamyl peptides alone or in combination with AST, ALT and methionine sulfoxide to discriminate each group from all other liver diseases and healthy controls. The solid and dashed curves represent the ROC curves for the training and validation cohorts, respectively. AUCt and AUCv in each panel indicate the AUC values in the training and validation cohorts, respectively. The group label indicates the discriminated group from all the other groups by an MLR model. The biomarkers in each panel were used in the MLR model for discriminating the group, e.g., ALT and γ-Glu-Taurine were the biomarkers for discriminating CNALT from the other groups. The coefficients and constant term of the MLR model of these biomarkers were summarized in Table 2.

acetaminophen (APAP)-treated mice [12], ophthalmate, a γ-glutamyl tripeptide, was synthesized through consecutive reactions with GCS and glutathione synthetase (GS), the same enzymes that play a role in GSH synthesis [12] (Fig. 5). Therefore, we investigated the alterations in the levels of hepatic amino acids, amines, γ-glutamyl dipeptides, and tripeptides after administration of buthionine sulfoximine (BSO), diethylmaleate (DEM) or APAP (Supplementary Fig. 4). BSO treatment resulted in GCS inhibition [20] and marked reductions in most of the hepatic γ-glutamyl dipeptide and tripeptide levels (Fig. 5 and Supplementary Fig. 4A). In contrast, DEM treatment led to GSH depletion by oxidation of the thiol group in GSH [21], resulting in GCS activation and considerable increases in the hepatic γ-glutamyl dipeptide and tripeptide levels compared with the controls (Fig. 5 and Supplementary Fig. 4A). The hepatic levels of several γ-glutamyl dipeptides and tripeptides were increased with concurrent GSH depletion in APAP-treated mice (Supplementary Fig. 4B and C). These results indicated that in mice, γ-glutamyl dipeptides and tripeptides were certainly synthesized via the ligation of glutamate by various amino acids through consecutive reactions with GCS and GS when GSH was depleted (Fig. 5). The identification details for the γ-glutamyl dipeptide biosynthetic pathway are described in the Supplementary data.

Discussion

Our analyses of 237 serum samples from patients with liver diseases and healthy controls revealed that γ-glutamyl dipeptides were increased in liver injuries and could provide specific information for different liver diseases. In APAP-induced liver injury in mice, ophthalmate, a γ-glutamyl tripeptide, was markedly increased as a byproduct of GSH synthesis [21] (Fig. 5 and Supplementary Fig. 4B). However, in liver diseases in humans, many γ-glutamyl dipeptides were primarily synthesized and secreted from hepatocytes into the blood (Figs. 1 and 5). Although the reason for the difference is unclear, it may be attributable to species differences in the levels and activities of enzymes and transporters [22,23].

In all types of liver disease, oxidative stress resulting from an imbalance between the production of reactive oxygen species (ROS) and the ability of a biological system to detoxify reactive intermediates plays a crucial role in the induction and progression of liver damage independently of its etiology [1]. In patients with hepatitis, oxidative stress is produced by inflammation induced by immunological mechanisms. Upon viral infection, NADPH oxidase produces ROS in neutrophils and macrophages, and ROS are also generated from free iron through the Fenton reaction [24–26]. ROS are further produced in hepatocytes upon

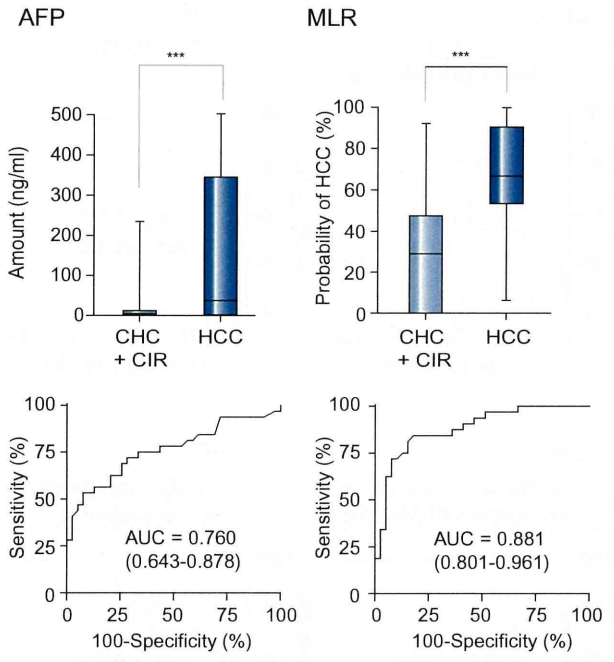

Fig. 4. Whisker box plots and ROC curves of AFP and MLR analyses based on γ-Glu-Ala, γ-Glu-Citrulline, γ-Glu-Thr and γ-Glu-Phe for discriminating patients with HCC (n = 32) from patients with CHC (n = 35) and CIR (n = 18).

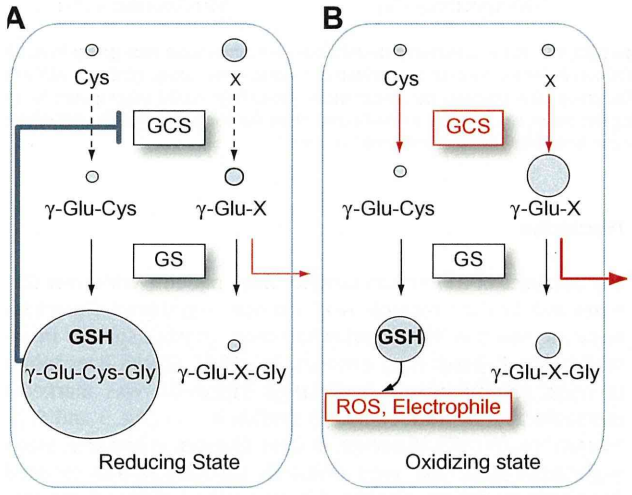

Fig. 5. Biosynthetic mechanism of γ-glutamyl peptides in hepatocytes under (A) reducing conditions and (B) oxidative stress. GCS is feedback-inhibited by GSH under reducing conditions and small amounts of γ-glutamyl dipeptides are synthesized. During oxidative stress, GSH is consumed, leading to GCS activation. This could result in biosynthesis of γ-glutamyl dipeptides, which are then effluxed across the hepatocellular membrane. γ-Glutamyl dipeptides and tripeptides are indicated by γ-Glu-X and Glu-X-Gly, respectively (X = amino acid or amine).

the release of inflammatory cytokines, such as tumor necrosis factor-α and interleukin-1β from inflammatory cells [27]. GSH is the most abundant antioxidant in hepatocytes, and helps to protect cells against ROS. Upon depletion of GSH, ROS induce oxidative stress resulting in liver damage, and reduced GSH levels have been demonstrated in various liver diseases [28–30].

Since γ-glutamyl dipeptides are byproducts of GSH synthesis catalyzed by GCS, their levels are indirect evidence for GSH production (Fig. 5). Different levels of γ-glutamyl dipeptides were observed in different types of liver disease and each γ-glutamyl dipeptide showed a somewhat different variation pattern among liver diseases (Fig. 2). This might be attributed to differences in hepatic levels of amino acids (the substrate of GCS) among liver diseases, though further studies are necessary to understand the details of this observation.

In healthy controls, the γ-glutamyl dipeptide levels were low. This occurred because under reducing conditions, the level of hepatic GSH was high and a small amount of GSH was biosynthesized (Fig. 5A). However, in the patients with liver diseases, GSH was consumed to neutralize the generated ROS, which in turn led to GCS activation, resulting in the biosynthesis of GSH together with γ-glutamyl dipeptides (Fig. 5B). Therefore, increased levels of γ-glutamyl dipeptides were observed in most liver injuries. Surprisingly, unlike AST and ALT, the levels of most γ-glutamyl dipeptides were markedly increased in asymptomatic individuals with AHB and CNALT (Fig. 2 and Supplementary Fig. 1), possibly because viral infection induced ROS generation followed by GSH depletion, which led to the biosynthesis of GSH and γ-glutamyl dipeptides (Fig. 5). We hypothesize that sufficiently high levels of GSH production neutralized ROS, resulting in lower incidences of AHB and CNALT.

There are relationships between liver diseases attributable to HCV infection and oxidative stress parameters, such as ROS, antioxidants, and inflammation. Oxidative stress increased with hepatic disease progression in HCV-infected patients [31]. Consistent with that report, among all the patients with HCV-related liver diseases, the serum levels of γ-glutamyl dipeptides, as indicators of hepatic GSH production, were markedly increased in CNALT and tended to decrease with disease progression (CNALT ⩾ CHC > CIR > HCC) (Fig. 2). These observations led us to conclude that at the time of viral infection (CNALT), a sufficient amount of GSH production can neutralize ROS and thus weaken the pathogenesis of liver damage. However, when GSH production falls below ROS generation, oxidative stress followed by inflammation is induced, resulting in the development and progression of liver diseases. Similarly, the levels of several γ-glutamyl dipeptides were significantly lower in NASH patients than in SS patients (Supplementary Fig. 3), indicating low levels of GSH production in NASH patients. Based on the present observations, we suggest that NASH is susceptible to oxidative stress and progression to liver fibrosis and cirrhosis.

HCC is one of the most common cancers in humans, and primarily develops in patients with chronic liver disease. Its early detection is important because effective treatments are available for the management of non-advanced cancers [32]. Until now, the diagnosis of HCC has relied on combinations of imaging techniques and measurements of the serum levels of AFP [33] and PIVKA-II [34]. Although they are reliable tumor markers for the diagnosis and monitoring of primary HCC, high levels of serum AFP and plasma PIVKA-II have also been observed in some gastric carcinomas [34,35]. However, the serum γ-glutamyl dipeptide levels in GC and HCC patients revealed significant differences, and the levels of several γ-glutamyl dipeptides was notably low in GC (Supplementary Fig. 2). We suspect that this occurred through differences in the tissue activities of the glutathione

system, since GSH is mainly synthesized *de novo* in the liver, and hypothesize that the γ-glutamyl dipeptide levels may reflect hepatic dysfunction.

Drug-induced hepatotoxicity is a frequent cause of liver injury, and the predominant clinical presentation is acute hepatitis and/or cholestasis. Overdoses of APAP, the most commonly used analgesic and antipyretic, can lead to possibly fatal hepatitis and several hundred deaths attributable to this drug occur annually in the United States. Our DI samples were from patients with so-called idiosyncratic hepatotoxicity, and the underlying mechanisms of this disease remain unclear. Interestingly, the changes in the serum levels of γ-glutamyl dipeptides were similar among the DI samples although the causative drugs differed widely and the mechanisms responsible for the development of hepatotoxicity may also be different. Our findings revealed that the amount of γ-glutamyl dipeptide production attributable to a reduction in the hepatocellular GSH concentration was a common feature in drug-induced idiosyncratic hepatotoxicity. With AUC values of 0.817 (training data) and 0.849 (validation data) (Supplementary Table 3), the serum levels of ALT and γ-Glu-Citrulline could be used to distinguish between DI patients on the one hand and patients with viral hepatitis infection and healthy controls on the other (Table 2). Therefore, we suggest that these compounds represent noninvasive biomarkers that facilitate rapid screening for DI.

In summary, our CE–TOFMS and LC–MS/MS metabolomics-based analyses of serum samples from patients with liver diseases showed quantitative differences in γ-glutamyl dipeptides in various liver diseases. Our highly specific set of γ-glutamyl dipeptides, transaminases, and methionine sulfoxide enabled us to discriminate among liver diseases including DI, AHB, CHB, CNALT, CHC, CIR, and HCC, indicating that they can be used as multiple biomarkers in rapid screening for different types and stages of liver disease. Furthermore, we have shown that γ-glutamyl dipeptide synthesis was catalyzed by GCS, the enzyme that is feedback-inhibited by GSH, and thus the levels of these biomarkers were indicative of hepatic GSH production. As observed in patients with HCV-related liver diseases and NAFLD, the serum γ-glutamyl dipeptide levels tended to decrease during the course of liver disease progression, indicating an increase in oxidative stress resulting from decreased GSH production during liver disease progression. Therefore, γ-glutamyl dipeptide measurement can potentially provide valuable information about the hepatic reduction–oxidation state to gain insights into the role of oxidative stress in the pathogenesis and progression of liver diseases.

Conflict of interest

The Authors who have taken part in this study declared that they do not have anything to disclose regarding funding or conflict of interest with respect to this manuscript.

Financial support

This work was supported by Health and Labour Sciences Research Grants "Research on Biological Markers for New Drug Development" (T.S.) and "Research on Risk of Chemical Substances" (T.S.). Additional support was obtained through grants from the Ministry of Education, Culture, Sports, Science and Technology (MEXT) for a Global COE Program entitled "Human Metabolomic Systems Biology" in Life Sciences (T.S., M.T. and M.S.) and the ERATO Gas Biology Project (M.S.), as well as research funds from the Yamagata Prefectural Government and City of Tsuruoka.

Supplementary data

Supplementary data associated with this article can be found, in the online version, at doi:10.1016/j.jhep.2011.01.031.

References

[1] Loguercio C, Federico A. Oxidative stress in viral and alcoholic hepatitis. Free Radic Biol Med 2003;34:1–10.
[2] Brunt EM. Nonalcoholic steatohepatitis. Semin Liver Dis 2004;24:3–20.
[3] Younossi ZM, Jarrar M, Nugent C, Randhawa M, Afendy M, Stepanova M, et al. A novel diagnostic biomarker panel for obesity-related nonalcoholic steatohepatitis (NASH). Obes Surg 2008;18:1430–1437.
[4] Piccinino F, Sagnelli E, Pasquale G, Giusti G. Complications following percutaneous liver biopsy. A multicentre retrospective study on 68,276 biopsies. J Hepatol 1986;2:165–173.
[5] Bolukbas C, Bolukbas FF, Horoz M, Aslan M, Celik H, Erel O. Increased oxidative stress associated with the severity of the liver disease in various forms of hepatitis B virus infection. BMC Infect Dis 2005;5:95.
[6] Sreekumar A, Poisson LM, Rajendiran TM, Khan AP, Cao Q, Yu J, et al. Metabolomic profiles delineate potential role for sarcosine in prostate cancer progression. Nature 2009;457:910–914.
[7] Bogdanov M, Matson WR, Wang L, Matson T, Saunders-Pullman R, Bressman SS, et al. Metabolomic profiling to develop blood biomarkers for Parkinson's disease. Brain 2008;131:389–396.
[8] Wang C, Kong H, Guan Y, Yang J, Gu J, Yang S, et al. Plasma phospholipid metabolic profiling and biomarkers of type 2 diabetes mellitus based on high-performance liquid chromatography/electrospray mass spectrometry and multivariate statistical analysis. Anal Chem 2005;77:4108–4116.
[9] Sabatine MS, Liu E, Morrow DA, Heller E, McCarroll R, Wiegand R, et al. Metabolomic identification of novel biomarkers of myocardial ischemia. Circulation 2005;112:3868–3875.
[10] Kenny LC, Dunn WB, Ellis DI, Myers J, Baker PN, Consortium TG, et al. Novel biomarkers for pre-eclampsia detected using metabolomics and machine learning. Metabolomics 2005;1:227–234.
[11] Soga T, Ohashi Y, Ueno Y, Naraoka H, Tomita M, Nishioka T. Quantitative metabolome analysis using capillary electrophoresis mass spectrometry. J Proteome Res 2003;2:488–494.
[12] Soga T, Baran R, Suematsu M, Ueno Y, Ikeda S, Sakurakawa T, et al. Differential metabolomics reveals ophthalmic acid as an oxidative stress biomarker indicating hepatic glutathione consumption. J Biol Chem 2006;281:16768–16776.
[13] Soga T, Igarashi K, Ito C, Mizobuchi K, Zimmermann HP, Tomita M. Metabolomic profiling of anionic metabolites by capillary electrophoresis mass spectrometry. Anal Chem 2009;81:6165–6174.
[14] Shintani T, Iwabuchi T, Soga T, Kato Y, Yamamoto T, Takano N, et al. Cystathionine beta-synthase as a carbon monoxide-sensitive regulator of bile excretion. Hepatology 2009;49:141–150.
[15] Goto S, Okuno Y, Hattori M, Nishioka T, Kanehisa M. LIGAND: database of chemical compounds and reactions in biological pathways. Nucleic Acids Res 2002;30:402–404.
[16] Kaneto H, Xu G, Song KH, Suzuma K, Bonner-Weir S, Sharma A, et al. Activation of the hexosamine pathway leads to deterioration of pancreatic beta-cell function through the induction of oxidative stress. J Biol Chem 2001;276:31099–31104.
[17] Levine RL, Berlett BS, Moskovitz J, Mosoni L, Stadtman ER. Methionine residues may protect proteins from critical oxidative damage. Mech Ageing Dev 1999;107:323–332.
[18] Babior BM. Phagocytes and oxidative stress. Am J Med 2000;109:33–44.
[19] Vogt W. Oxidation of methionyl residues in proteins: tools, targets, and reversal. Free Radic Biol Med 1995;18:93–105.
[20] Griffith OW, Meister A. Potent and specific inhibition of glutathione synthesis by buthionine sulfoximine (*S-n*-butyl homocysteine sulfoximine). J Biol Chem 1979;254:7558–7560.
[21] Zalups RK, Lash LH. Depletion of glutathione in the kidney and the renal disposition of administered inorganic mercury. Drug Metab Dispos 1997;25:516–523.

[22] Ishizuka H, Konno K, Shiina T, Naganuma H, Nishimura K, Ito K, et al. Species differences in the transport activity for organic anions across the bile canalicular membrane. J Pharmacol Exp Ther 1999;290:1324–1330.
[23] Mainwaring GW, Williams SM, Foster JR, Tugwood J, Green T. The distribution of theta-class glutathione *S*-transferases in the liver and lung of mouse, rat and human. Biochem J 1996;318:297–303.
[24] Marrogi AJ, Khan MA, van Gijssel HE, Welsh JA, Rahim H, Demetris AJ, et al. Oxidative stress and p53 mutations in the carcinogenesis of iron overload-associated hepatocellular carcinoma. J Natl Cancer Inst 2001;93:1652–1655.
[25] Toyokuni S, Okamoto K, Yodoi J, Hiai H. Persistent oxidative stress in cancer. FEBS Lett 1995;358:1–3.
[26] Sutton A, Nahon P, Pessayre D, Rufat P, Poire A, Ziol M, et al. Genetic polymorphisms in antioxidant enzymes modulate hepatic iron accumulation and hepatocellular carcinoma development in patients with alcohol-induced cirrhosis. Cancer Res 2006;66:2844–2852.
[27] Koike K, Miyoshi H. Oxidative stress and hepatitis C viral infection. Hepatol Res 2006;34:65–73.
[28] Boya P, de la Pena A, Beloqui O, Larrea E, Conchillo M, Castelruiz Y, et al. Antioxidant status and glutathione metabolism in peripheral blood mononuclear cells from patients with chronic hepatitis C. J Hepatol 1999;31:808–814.
[29] Tanyalcin T, Taskiran D, Topalak O, Batur Y, Kutay F. The effects of chronic hepatitis C and B virus infections on liver reduced and oxidized glutathione concentrations. Hepatol Res 2000;18:104–109.
[30] Moriya K, Nakagawa K, Santa T, Shintani Y, Fujie H, Miyoshi H, et al. Oxidative stress in the absence of inflammation in a mouse model for hepatitis C virus-associated hepatocarcinogenesis. Cancer Res 2001;61:4365–4370.
[31] Sumida Y, Nakashima T, Yoh T, Nakajima Y, Ishikawa H, Mitsuyoshi H, et al. Serum thioredoxin levels as an indicator of oxidative stress in patients with hepatitis C virus infection. J Hepatol 2000;33:616–622.
[32] Bruix J. Treatment of hepatocellular carcinoma. Hepatology 1997;25:259–262.
[33] Szklaruk J, Silverman PM, Charnsangavej C. Imaging in the diagnosis, staging, treatment, and surveillance of hepatocellular carcinoma. Am J Roentgenol 2003;180:441–454.
[34] Kudo M, Takamine Y, Nakamura K, Shirane H, Uchida H, Kasakura S, et al. Des-gamma-carboxy prothrombin (PIVKA-II) and alpha-fetoprotein-producing IIc-type early gastric cancer. Am J Gastroenterol 1992;87: 1859–1862.
[35] Takano S, Honda I, Watanabe S, Soda H, Nagata M, Hoshino I, et al. PIVKA-II-producing advanced gastric cancer. Int J Clin Oncol 2004;9:330–333.

Association of Gene Expression Involving Innate Immunity and Genetic Variation in Interleukin 28B With Antiviral Response

Yasuhiro Asahina,[1] Kaoru Tsuchiya,[1] Masaru Muraoka,[1,2] Keisuke Tanaka,[1,2] Yuichiro Suzuki,[1,2] Nobuharu Tamaki,[1] Yoshihide Hoshioka,[1] Yutaka Yasui,[1] Tomoji Katoh,[1] Takanori Hosokawa,[1] Ken Ueda,[1] Hiroyuki Nakanishi,[1] Jun Itakura,[1] Yuka Takahashi,[1] Masayuki Kurosaki,[1] Nobuyuki Enomoto,[2] Sayuri Nitta,[3] Naoya Sakamoto,[3] and Namiki Izumi[1]

Innate immunity plays an important role in host antiviral response to hepatitis C viral (HCV) infection. Recently, single nucleotide polymorphisms (SNPs) of *IL28B* and host response to peginterferon α (PEG-IFNα) and ribavirin (RBV) were shown to be strongly associated. We aimed to determine the gene expression involving innate immunity in *IL28B* genotypes and elucidate its relation to response to antiviral treatment. We genotyped *IL28B* SNPs (rs8099917 and rs12979860) in 88 chronic hepatitis C patients treated with PEG-IFNα-2b/RBV and quantified expressions of viral sensors (*RIG-I, MDA5*, and *LGP2*), adaptor molecule (*IPS-1*), related ubiquitin E3-ligase (*RNF125*), modulators (*ISG15* and *USP18*), and *IL28* (*IFNλ*). Both *IL28B* SNPs were 100% identical; 54 patients possessed rs8099917 TT/rs12979860 CC (*IL28B* major patients) and 34 possessed rs8099917 TG/rs12979860 CT (*IL28B* minor patients). Hepatic expressions of viral sensors and modulators in *IL28B* minor patients were significantly up-regulated compared with that in *IL28B* major patients (≈3.3-fold, $P < 0.001$). However, expression of *IPS-1* was significantly lower in *IL28B* minor patients (1.2-fold, $P = 0.028$). Expressions of viral sensors and modulators were significantly higher in nonvirological responders (NVR) than that in others despite stratification by *IL28B* genotype (≈2.6-fold, $P < 0.001$). Multivariate and ROC analyses indicated that higher *RIG-I* and *ISG15* expressions and *RIG-I/IPS-1* expression ratio were independent factors for NVR. IPS-1 down-regulation in *IL28B* minor patients was confirmed by western blotting, and the extent of IPS-1 protein cleavage was associated with the variable treatment response. *Conclusion:* Gene expression involving innate immunity is strongly associated with *IL28B* genotype and response to PEG-IFNα/RBV. Both *IL28B* minor allele and higher *RIG-I* and *ISG15* expressions and *RIG-I/IPS-1* ratio are independent factors for NVR. (HEPATOLOGY 2012;55:20-29)

Infection with hepatitis C virus (HCV) is a common cause of chronic hepatitis, which progresses to liver cirrhosis and hepatocellular carcinoma in many patients.[1] Pegylated interferon α (PEG-IFNα) and ribavirin (RBV) combination therapy has been used to treat chronic hepatitis C (CH-C) to alter the natural course of this disease. However, 20% patients are nonvirological responders (NVR) whose HCV-RNA does not become negative during the 48 weeks of PEG-IFNα/RBV combination therapy.[2] In a recent genome-wide association study, single nucleotide polymorphisms (SNPs) located near interleukin 28B

Abbreviations: CH-C, chronic hepatitis C; γ-GTP, γ-glutamyl transpeptidase; GAPDH, glyceraldehyde-3-phosphate dehydrogenase; HCV, hepatitis C virus; HMBS, hydroxymethylbilane synthase; IL28, interleukin 28; IPS-1, IFNβ promoter stimulator 1; ISG15, interferon-stimulated gene 15; MDA5, melanoma differentiation associated gene 5; NVR; nonvirological responders; PEG-IFNα, pegylated interferonα; SNP, single nucleotide polymorphism; RIG-I, retinoic acid-inducible gene I; RBV, ribavirin; RNF125, ring-finger protein 125; ROC, receiver operator characteristic; SVR, sustained viral responder; TVR, transient virological responder; USP18, ubiquitin-specific protease 18; VR, virological responder.

From the [1]Department of Gastroenterology and Hepatology, Musashino Red Cross Hospital, Tokyo, Japan; [2]First Department of Internal Medicine, Faculty of Medicine, University of Yamanashi, Yamanashi, Japan; [3]Department of Gastroenterology and Hepatology, Tokyo Medical and Dental University, Tokyo, Japan.

Received May 14, 2011; accepted August 16, 2011.

Supported by grants from the Japanese Ministry of Education, Culture, Sports, Science and Technology and the Japanese Ministry of Welfare, Health and Labor. The funding source had no role in the collection, analysis, or interpretation of the data, or in the decision to submit the article for publication.

(*IL28B*) that encodes for type III IFNλ3 were shown to be strongly associated with a virological response to PEG-IFNα/RBV combination therapy.[3-5] In particular, the rs8099917 TG and GG genotypes were shown to be strongly associated with a null virological response to PEG-IFNα/RBV.[3] However, mechanisms involving resistance to PEG-IFNα/RBV have not been completely elucidated.

The innate immune system has an essential role in host antiviral defense against HCV infection.[6] The retinoic acid-inducible gene I (RIG-I), a cytoplasmic RNA helicase, and related melanoma differentiation associated gene 5 (MDA5) play essential roles in initiating the host antiviral response by detecting intracellular viral RNA.[7,8] The IFNβ promoter stimulator 1 (IPS-1)—also called the caspase-recruiting domain adaptor inducing IFNβ, mitochondrial antiviral signaling protein, or virus-induced signaling adaptor—is an adaptor molecule. IPS-1 connects RIG-I sensing to downstream signaling, resulting in *IFNβ* gene activation.[9-12] RIG-I sensing of incoming viral RNA has been shown to be modified by LGP2,[8,13] a helicase related to RIG-I and MDA5 lacking caspase-recruiting domain. The ubiquitin ligase ring-finger protein 125 (RNF125) has been shown to conjugate ubiquitin to RIG-I, MDA5, and IPS-1 and this suppresses the functions of these proteins.[14] Further, these molecules are ISGylated by the IFN-stimulated gene 15 (ISG15), a ubiquitin-like protein,[15] and ISG15 is specifically removed from ISGylated protein by ubiquitin-specific protease 18 (USP18) to regulate the RIG-I/IPS-1 system.[16,17] Moreover, the NS3/4A protease of HCV specifically cleaves IPS-1 as part of its immune-evasion strategy.[9,18] Therefore, the RIG-I/IPS-1 system and its regulatory systems have essential roles in the innate antiviral response.

Recently, we demonstrated that baseline intrahepatic gene expression levels of the RIG-I/IPS-1 system were prognostic biomarkers of the final virological outcome in CH-C patients who were treated with PEG-IFNα/RBV combination therapy.[19] We found that up-regulation of *RIG-I* and *ISG15* and a higher expression ratio of *RIG-I/IPS-1* could predict NVR for subsequent treatment with PEG-IFNα/RBV combination therapy.[19] However, association of gene expression involving innate immunity and genetic variation of *IL28B* has not yet been elucidated. Hence, the aim of this study was to determine gene expression involving the innate immune system in different genetic variations of *IL28B* and elucidate the relation of gene expression to final virological outcome of PEG-IFNα/RBV combination therapy in CH-C patients.

Patients and Methods

Patients. Among histologically proven CH-C patients admitted at the Musashino Red Cross Hospital, 88 patients with HCV genotype 1b and a high viral load (>5 log IU/mL by TaqMan HCV assay; Roche Molecular Diagnostics, Tokyo, Japan) were included in the present study (Table 1). Patients with decompensated liver cirrhosis, autoimmune hepatitis, or alcoholic liver injury were excluded. No patient had tested positive for hepatitis B surface antigen or anti-human immunodeficiency virus antibody or had received immunomodulatory therapy before enrollment. Forty-two patients had been enrolled in a previous study that determined hepatic gene expression involving innate immunity.[19] Written informed consent was obtained from all patients and the study was approved by the Ethical Committee of Musashino Red Cross Hospital in accordance with the Declaration of Helsinki.

Treatment Protocol. The patients were administered subcutaneous injections of PEG-IFNα-2b (PegIntron, MSD, Whitehouse Station, NJ) at a dose of 1.5 $\mu g\ kg^{-1}\ week^{-1}$ for 48 weeks. RBV (Rebetol, MSD) was administered concomitantly over this treatment period, administered orally twice daily at 600 mg/day for patients who weighed less than 60 kg and 800 mg/day for patients who weighed between 60-80 kg. The dose of PEG-IFNα-2b was reduced to 0.75 $\mu g\ kg^{-1}\ week^{-1}$ when either neutrophil count was less than $750/mm^3$ or platelet count was less than $80 \times 10^3/mm^3$. The dose of RBV was reduced to 600 mg/day when the hemoglobin concentration decreased to 10 g/dL. More than 80% adherence was achieved in all patients.

Measurement of Hepatic Gene Expression. Liver biopsy was performed immediately before initiating

Address reprint requests to: Naoki Izumi, M.D., Ph.D., Chief, Department of Gastroenterology and Hepatology, Musashino Red Cross Hospital, 1-26-1 Kyonancho 1-26-1, Musashinoshi, Tokyo 180-8610, Japan. E-mail: nizumi@musashino.jrc.or.jp; fax: +81-422-32-9551.

View this article online at wileyonlinelibrary.com.

DOI 10.1002/hep.24623

Potential conflict of interest: Nothing to report.

Additional Supporting Information may be found in the online version of this article.